DEPARTMENT OF ELECTRONICS AND TELECOMMUNICATION ENGINEERING

JABALPUR ENGINEERING COLLEGE, JABALPUR

GOKALPUR, JABALPUR– 482011

A Project Report on

"MICROSTRIP PATCH ANTENNA"

SUBMITTED TO

JABALPUR ENGINEERING COLLEGE, JABALPUR

Submitted in partial fulfillment of the requirements for the award of graduate degree of

BACHELOR OF TECHNOLOGY

IN

ELECTRONICS AND TELECOMMUNICATION ENGINEERING

SUBMITTED BY

RISHAV PANDEY (0201EC181066)

RITESH SINGH (0201EC181067)

ROHIT GUPTA (0201EC181068)

ROSHIT KARNAVADIYA(0201EC181070)

SAKSHI DHARMANI (0201EC181073)

UNDER THE GUIDANCE OF

PROF. GARIMA TIWARI

DEPARTMENT OF ELECTRONICS AND TELECOMMUNICATION ENGINEERING

8TH SEMESTER

DEPARTMENT OF ELECTRONICS AND TELECOMMUNICATION ENGINEERING

SESSION (APRIL 2022)

DEPARTMENT OF ELECTRONICS AND TELECOMMUNICATION ENGINEERING

JABALPUR ENGINEERING COLLEGE, JABALPUR

GOKALPUR, JABALPUR– 482011

A Project Report on

"MICROSTRIP PATCH ANTENNA"

SUBMITTED TO

JABALPUR ENGINEERING COLLEGE, JABALPUR

Submitted in partial fulfillment of the requirements for the award of graduate degree of

BACHELOR OF TECHNOLOGY

IN

ELECTRONICS AND TELECOMMUNICATION ENGINEERING

SUBMITTED BY

RISHAV PANDEY (0201EC181066)

RITESH SINGH (0201EC181067)

ROHIT GUPTA (0201EC181068)

ROSHIT KARNAVADIYA (0201EC181070)

SAKSHI DHARMANI (0201EC181073)

UNDER THE GUIDANCE OF

PROF. GARIMA TIWARI

DEPARTMENT OF ELECTRONICS AND TELECOMMUNICATION ENGINEERING

8TH SEMESTER

DEPARTMENT OF ELECTRONICS AND TELECOMMUNICATION ENGINEERING

SESSION (APRIL 2022)

DEPARTMENT OF ELECTRONICS AND TELECOMMUNICATIONENGINEERING

JABALPUR ENGINEERING COLLEGE, JABALPUR

GOKALPUR, JABALPUR 482011

DECLARATION

We hereby declare that the project report entitled "MICROSTRIP PATCH ANTENNA" submitted by us in partial fulfillment of the requirement for the award of BACHELOR OF TECHNOLOGY by RAGIV GANDHI PRODYOGIKI VISHWAVIDYALAYA, BHOPAL is authentic work undertaken by us.

We further declare that the work reported in this project has not been submitted and will not be submitted, either in part or in full, for the award of any other degree or diploma in this institute or any other institute or university.

SUBMITTED BY

RISHAV PANDEY (0201EC181066)

RITESH SINGH (0201EC181067)

ROHIT GUPTA (0201EC181068)

ROSHIT KARNAVADIYA (0201EC181070)

SAKSHI DHARMANI (0201EC181073)

DEPARTMENT OF ELECTRONICS AND TELECOMMUNICATIONENGINEERING

JABALPUR ENGINEERING COLLEGE, JABALPUR

GOKALPUR, JABALPUR 482011

CERTIFICATE

ACADEMIC YEAR 2021-22

This is to certify that the project planning entitled "MICROSTRIP PATCH ANTENNA" submitted by RISHAV PANDEY (0201EC181066), RITESH SINGH (0201EC181067), ROHIT GUPTA (0201EC181068), ROSHIT KARNAVDIYA (0201EC181070), SAKSHI DHARMANI (0201EC181073) is approved for submission towards Partial fulfillment of the requirement for the award of degree of BACHELOR OF TECHNOLOGY in ELECTRONICS AND TELECOMMUNICATION ENGINEERING from JABALPUR ENGINEERING COLLEGE, JABALPUR (M.P.).

INTERNAL EXAMINER

DATE:

EXTERNAL EXAMINER

DATE:

DEPARTMENT OF ELECTRONICS AND TELECOMMUNICATIONENGINEERING

JABALPUR ENGINEERING COLLEGE, JABALPUR

GOKALPUR, JABALPUR 482011

CERTIFICATE

This is to certify that the project planning entitled "MICROSTRIP PATCH ANTENNA" submitted by RISHAV PANDEY (0201EC181066), RITESH SINGH (0201EC181067), ROHIT GUPTA (0201EC181068), ROSHIT KARNAVDIYA(0201EC181070), SAKSHI DHARMANI (0201EC181073) has been carried out under my Guidance and Supervision. The project is approved for submission towards Partial fulfillment of the requirement for the award of degree ofBACHELOR OF TECHNOLOGY in ELECTRONICS AND TELECOMMUNICATION ENGINEERING from JABALPUR ENGINEERING COLLEGE, JABALPUR (M.P.).

DR. BHAVANA JHARIA

Head of Department
Electronics and
Telecommunications Department

DEPARTMENT OF ELECTRONICS AND TELECOMMUNICATION ENGINEERING

JABALPUR ENGINEERING COLLEGE, JABALPUR

GOKALPUR, JABALPUR– 482011

ACKNOWLEDGEMENT

It is our proud privilege and duty to express our sincere regards to several people for the kind of help and guidance received from them in preparation of this report. It would not have been possible to prepare this report in this form without their valuable help, cooperation and guidance.

First and foremost, we wish to record our sincere gratitude to Dr. Bhavana Jharia, Head, Department of Electronics and Telecommunication Engineering, JEC, for her valuable suggestions and guidance throughout the period of my report. Our numerous discussions with her were extremely helpful.

We are grateful to our Principal, Dr. A.K. SHARMA, Principal, Jabalpur Engineering College, Jabalpur for his constant support and encouragement in preparation of this report and for making available library and laboratory facilities needed to prepare this report.

We take this opportunity to thank Prof. Amit Baghel, Asst Prof. Garima Tiwari, Prof Agya Mishra and all faculties of our Department of Electronics and Telecommunication Engineering, JEC Jabalpur for guiding us in investigations forthis report and in carrying out experimental work.

RISHAV PANDEY (0201EC181066)
RITESH SINGH (0201EC181067)
ROHIT GUPTA (0201EC181068)
ROSHIT KARNAVDIYA (0201EC181070)
SAKSHI DHARMANI (0201EC181073)

Contents

1. MICROSTRIP ANTENNAS

INTRODUCTION:

In high-performance aircraft, spacecraft, satellite, and missile applications, where size, weight, cost, performance, ease of installation, and aerodynamic profile are constraints, low-profile antennas may be required. Presently there are many other governments and commercial applications, such as mobile radio and wireless communications, that have similar specifications. To meet these requirements, microstrip antennas can be used. These antennas are low profile, conformable to planar and nonplanar surfaces, simple and inexpensive to manufacture using modern printed-circuit technology, mechanically robust when mounted on rigid surfaces, compatible with MMIC designs, and when the particular patch shape and mode are selected, they are very versatile in terms of resonant frequency, polarization, pattern, and impedance. In addition, by adding loads between the patch and the ground plane, such as pins and varactor diodes, adaptive elements with variable resonant frequency, impedance, polarization, and pattern can be designed .

Major operational disadvantages of microstrip antennas are their low efficiency, low power, high Q (sometimes in excess of 100), poor polarization purity, poor scan performance, spurious feed radiation and very narrow frequency bandwidth, which is typically only a fraction of a percent or at most a few percent. In some applications, such as in government security systems, narrow bandwidths are desirable. However, there are methods, such as increasing the height of the substrate, that can be used to extend the efficiency (to as large as 90 percent if surface waves are not included) and bandwidth (up to about 35 percent) . However, as the height increases, surface waves are introduced which usually are not desirable because they extract power from the total available for direct radiation(space waves). The surface waves travel within the substrate and they are scattered at bends and surface discontinuities, such as the truncation of the dielectric and ground plane , and degrade the antenna pattern and polarization characteristics. Surface waves can be eliminated, while maintaining large bandwidths, by using cavities . Stacking, as well as other methods, of microstrip elements can also be used to increase the bandwidth . In

frequencies outside the operating band, are rather large physically at VHF and possibly UHF frequencies, and in large arrays there is a trade-off between bandwidth and scan volume.

1.1 Basic Characteristics

Microstrip antennas received considerable attention starting in the 1970s, although the idea of a microstrip antenna can be traced to 1953 and a patent in 1955 .
Microstrip antennas, as shown in Figure 1(a), consist of a very thin (t _ $\lambda 0$, where $\lambda 0$ is the free-space wavelength) metallic strip (patch) placed a small fraction of a wavelength (h _ $\lambda 0$, usually $0.003\lambda 0 \leq h \leq 0.05\lambda 0$) above a ground plane. The microstrip patch is designed so its pattern maximum is normal to the patch (broadside radiator). This is accomplished by properly choosing the mode (field configuration) of excitation beneath the patch. End-fire radiation can also be accomplished by judicious mode selection. For a rectangular patch, the length L of the element is usually $\lambda 0/3 < L < \lambda 0/2$.
The strip (patch) and the ground plane are separated by a dielectric sheet (referred to as the substrate), as shown in Figure 1(a).
There are numerous substrates that can be used for the design of microstrip antennas, and their dielectric constants are usually in the range of $2.2 \leq Ir \leq 12$. The ones that are most desirable for good antenna performance are thick substrates whose dielectric constant is in the lower end of the range because they provide better efficiency, larger bandwidth, loosely bound fields for radiation into space, but at the expense of larger element size . Thin substrates with higher dielectric constants are desirable for microwave circuitry because they require tightly bound fields to minimize undesired radiation and coupling, and lead to smaller element sizes; however, because of their

greater losses, they are less efficient and have relatively smaller bandwidths. Since

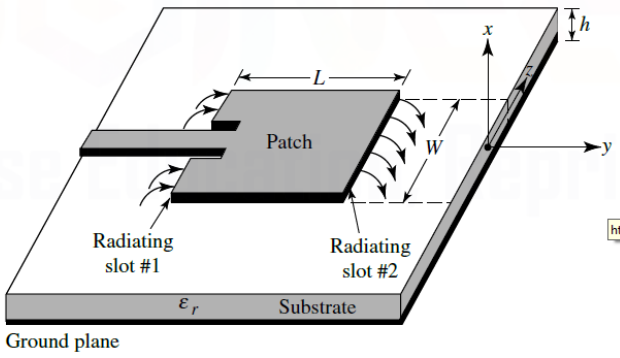

(a) Microstrip antenna

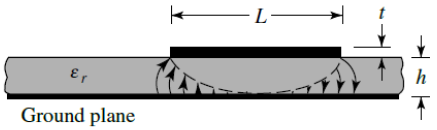

(b) Side view

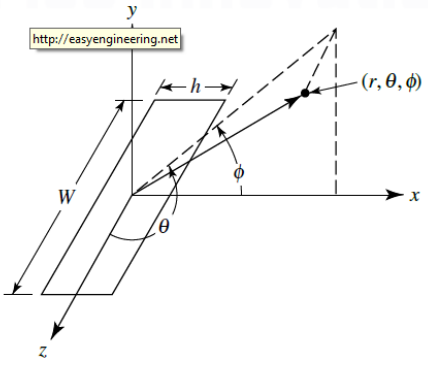

(c) Coordinate system for each radiating slot

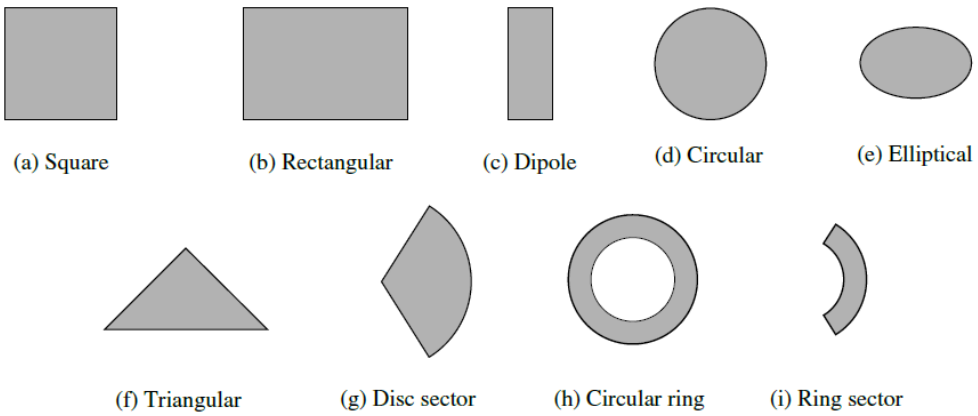

microstrip antennas are often integrated with other microwave circuitry, a compromise has to be reached between good antenna performance and circuit design.
Often microstrip antennas are also referred to as *patch* antennas. The radiating elements and the feed lines are usually photoetched on the dielectric substrate. The radiating patch may be square, rectangular, thin strip (dipole), circular, elliptical, triangular, or any other configuration. These and others are illustrated in Figure 2.
Square, rectangular, dipole (strip), and circular are the most common because of ease of analysis and fabrication, and their attractive radiation characteristics, especially low cross-polarization radiation. Microstrip dipoles are attractive because they inherently possess a large bandwidth and occupy less space, which makes them attractive for arrays . Linear and circular polarizations can be achieved with
either single elements or arrays of microstrip antennas. Arrays of microstrip elements, with single or multiple feeds, may also be used to introduce scanning capabilities and achieve greater directivities. These will be discussed inlater sections.

1.2 Feeding Methods

There are many configurations that can be used to feed microstrip antennas. The four most popular are the microstrip line, coaxial probe, aperture coupling, and proximity coupling. These are displayed in Figure 3. One
set of equivalent circuits for each one of these is shown in Figure 4. The microstrip feed line is also a conducting strip, usually of much smaller width compared to the patch. The microstrip-line feed is easy to fabricate, simple to match by controlling the inset position and rather simple to model. However, as the substrate thickness increases, surface waves and spurious feed radiation increase, which for practical designs limit the bandwidth (typically 2–5%).
Coaxial-line feeds, where the inner conductor of the coax is attached to the radiation patch while the outer conductor is connected to the ground plane, are also widely used. The coaxial probe feed is also easy to fabricate and match, and it has low spurious

radiation. However, it also has narrow bandwidth and it is more difficult to model, especially for thick substrates ($h > 0.02\lambda 0$).
Both the microstrip feed line and the probe possess inherent asymmetries which generate higher order modes which produce cross-polarized radiation. To overcome some of these problems, noncontacting aperture-coupling feeds, as shown in Figures 3(c, d),

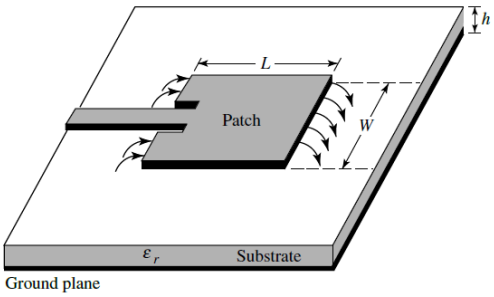

(a) Microstrip line feed

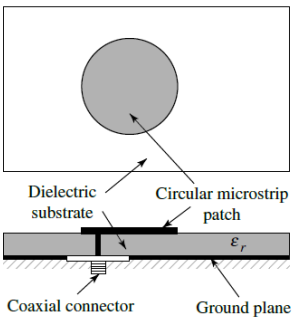

(b) Probe feed

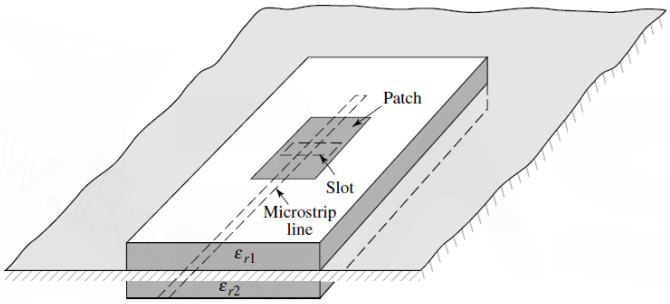

(c) Aperture-coupled feed

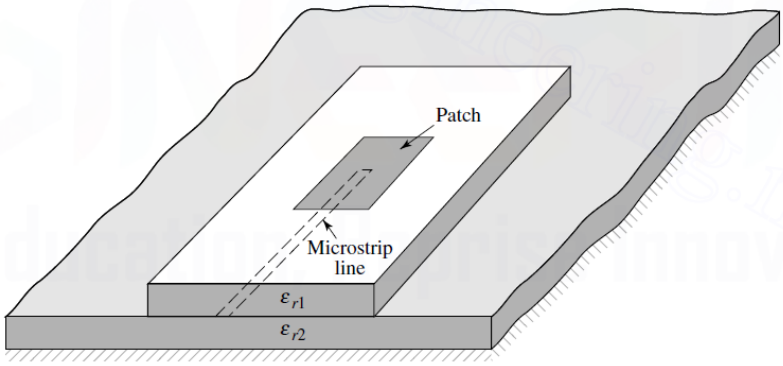

(d) Proximity-coupled feed

have been introduced. The aperture coupling of Figure 3(c) is the most difficult of all four to fabricate and it also has narrow bandwidth. However, it is somewhat easier to model and has moderate spurious radiation. The aperture coupling consists of two substrates separated by a ground plane. On the bottom side of the lower substrate there is a microstrip feed line whose energy is coupled to the patch through a slot on the ground

plane separating the two substrates. This arrangement allows independent optimization

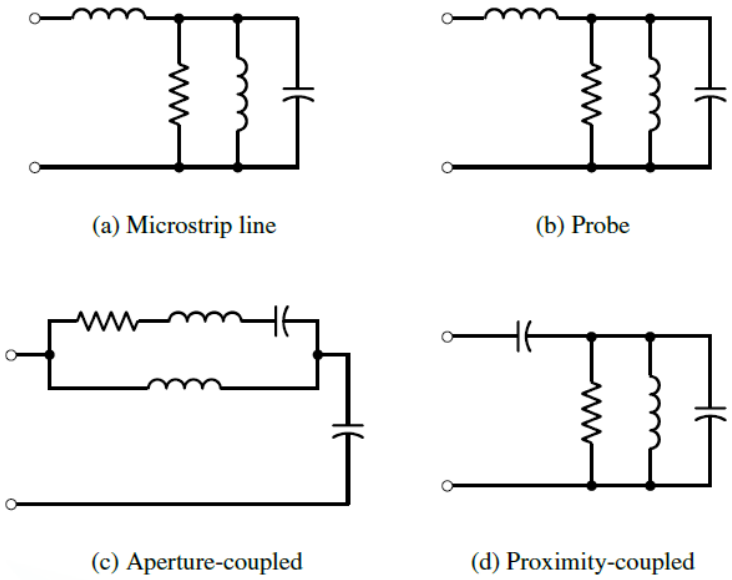

of the feed mechanism and the radiating element. Typically a high dielectric material is used for the bottom substrate, and thick low dielectric constant material for the top substrate. The ground plane between the substrates also isolates the feed from the radiating element and minimizes interference of spurious radiation for pattern formation and polarization purity. For this design, the substrate electrical parameters, feed line width, and slot size and position can be used to optimize the design . Typically matching is performed by controlling the width of the feed line and the length of the slot. The coupling through the slot can be modeled using the theory of Bethe , which is also used to account for coupling through a small aperture in a conducting plane. This theory has been successfully used to analyze waveguide couplers using coupling through holes . In this theory the slot is represented by an equivalent normal electric dipole to account for the normal component (to the slot) of the electric field, and an equivalent horizontal magnetic dipole to account for the tangential component (to the slot) magnetic field. If the slot is centered below the patch, where ideally for the dominant mode the electric field is zero while the magnetic field is maximum, the magnetic coupling will dominate. Doing this also leads to good polarization purity and no cross-polarized radiation in the principal planes . Of the four feeds described here, the proximity coupling has the largest bandwidth (as high as 13 percent), is somewhat easy to model and has low spurious radiation. However its fabrication is somewhat more difficult. The length of the feeding stub and the width-to-line ratio of the patch can be used to control the match .

1.3 Methods of Analysis

There are many methods of analysis for microstrip antennas. The most popular models

are the *transmission-line cavity* , and *full wave*
(which include primarily integral equations/Moment Method)
The transmission-line model is the easiest of all, it gives good physical insight, but is less accurate and it is more difficult to model coupling Compared to the transmission-line model, the cavity model is more accurate but at the same time more complex. However, it also gives good physical insight and is rather difficult to model coupling, although it has been used successfully In general when applied
properly, the full-wave models are very accurate, very versatile, and can treat single elements, finite and infinite arrays, stacked elements, arbitrary shaped elements, and coupling. However they are the most complex models and usually give less physical insight. In this chapter we will cover the transmission-line and cavity models only. However results and design curves from full-wave models will also be included. Since they are the most popular and practical, in this chapter the only two patch configurations that will be considered are the rectangular and circular. Representative radiation characteristics of some other configurations will be included.

2. RECTANGULAR PATCH

The rectangular patch is by far the most widely used configuration. It is very easy to analyze using both the transmission-line and cavity models, which are most accurate for thin substrates . We begin with the transmission-line model because it is easier to illustrate.

2.1 Transmission-Line Model

It was indicated earlier that the transmission-line model is the easiest of all but it yields the least accurate results and it lacks the versatility. However, it does shed some physical insight. As it will be demonstrated in Section 2.2 using the cavity model, a rectangular microstrip antenna can be represented as an array of two *radiating* narrow apertures (slots), each of width W and height h, separated by a distance L. Basically the transmission-line model represents the microstrip antenna by two slots, separated by a low-impedance Zc transmission line of length L.

A. Fringing Effects

Because the dimensions of the patch are finite along the length and width, the fields at the edges of the patch undergo fringing. This is illustrated along the length in Figures 1(a,b) for the two radiating slots of the microstrip antenna. The same applies along the width. The amount of fringing is a function of the dimensions of the patch and the height of the substrate. For the principal E-plane (xy-plane) fringing is a function of the ratio of the length of the patch L to the height h of the substrate (L/h) and the dielectric constant Ir of the substrate. Since for microstrip antennas L/h _ 1, fringing is reduced; however, it must be taken into account because it influences the resonant frequency of the antenna. The same applies for the width.

For a microstrip line shown in Figure 5(a), typical electric field lines are shown in Figure 5(b). This is a nonhomogeneous line of two dielectrics; typically the substrate and air. As can be seen, most of the electric field lines reside in the substrate and parts of some lines exist in air. As W/h _ 1 an dIr _ 1, the electric field lines concentrate mostly in the substrate. Fringing in this case makes the microstrip line look wider electrically compared to its physical dimensions. Since some of the waves travel inthe substrate and some inair, an *effective dielectric constant* Ireff is introduced to

account for fringing and the wave propagation in the line.
To introduce the effective dielectric constant, let us assume that the center conductor of the microstrip line with its original dimensions and height above the ground plane

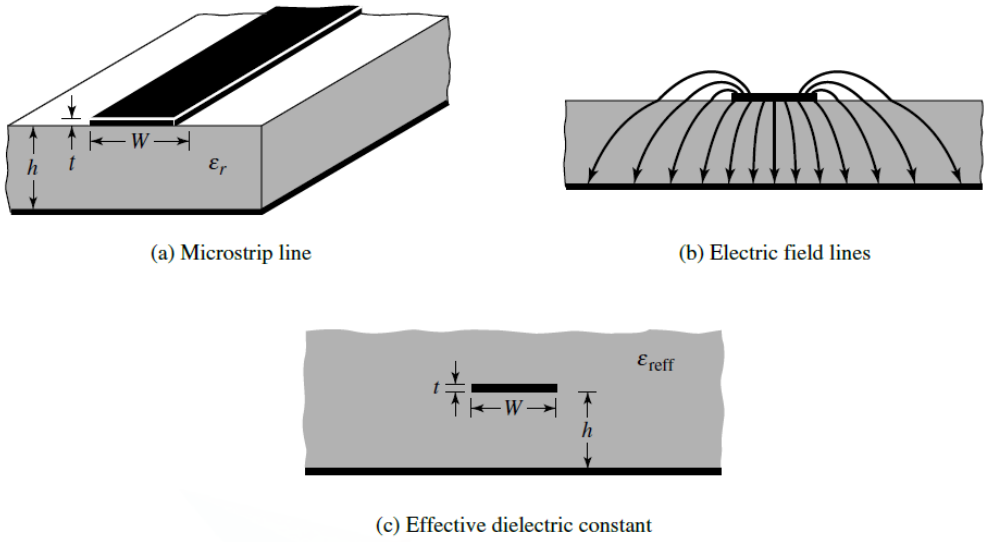

(a) Microstrip line

(b) Electric field lines

(c) Effective dielectric constant

is embedded into one dielectric, as shown in Figure 5(c). The effective dielectric constant is defined *as the dielectric constant of the uniform dielectric material so that the line of Figure 5(c) has identical electrical characteristics, particularly propagation constant, as the actual line of Figure 5(a)*. For a line with air above the substrate, the effective dielectric constant has values in the range of $1 < I\text{reff} < Ir$. For most applications where the dielectric constant of the substrate is much greater than unity (Ir _ 1), the value of Ireff will be closer to the value of the actual dielectric constant Ir of the substrate. The effective dielectric constant is also a function of frequency. As the frequency of operation increases, most of the electric field lines concentrate in the substrate. Therefore the microstrip line behaves more like a homogeneous line of one dielectric (only the substrate), and the effective dielectric constant approaches the value of the dielectric constant of the substrate. Typical variations, as a function of frequency, of the effective dielectric constant for a microstrip line with three different substrates are shown in Figure 6.
For low frequencies the effective dielectric constant is essentially constant. At intermediate frequencies its values begin to monotonically increase and eventually approach the values of the dielectric constant of the substrate. The initial values (at low frequencies) of the effective dielectric constant are referred to as the *static values*, and they are givenby [

$$W/h > 1$$

$$\epsilon_{\text{reff}} = \frac{\epsilon_r + 1}{2} + \frac{\epsilon_r - 1}{2}\left[1 + 12\frac{h}{W}\right]^{-1/2}$$

B. Effective Length, Resonant Frequency, and Effective Width

Because of the fringing effects, electrically the patch of the microstrip antenna looks greater than its physical dimensions. For the principal *E*-plane (*xy*-plane), this is demonstrated in Figure 7 where the dimensions of the patch along its length have

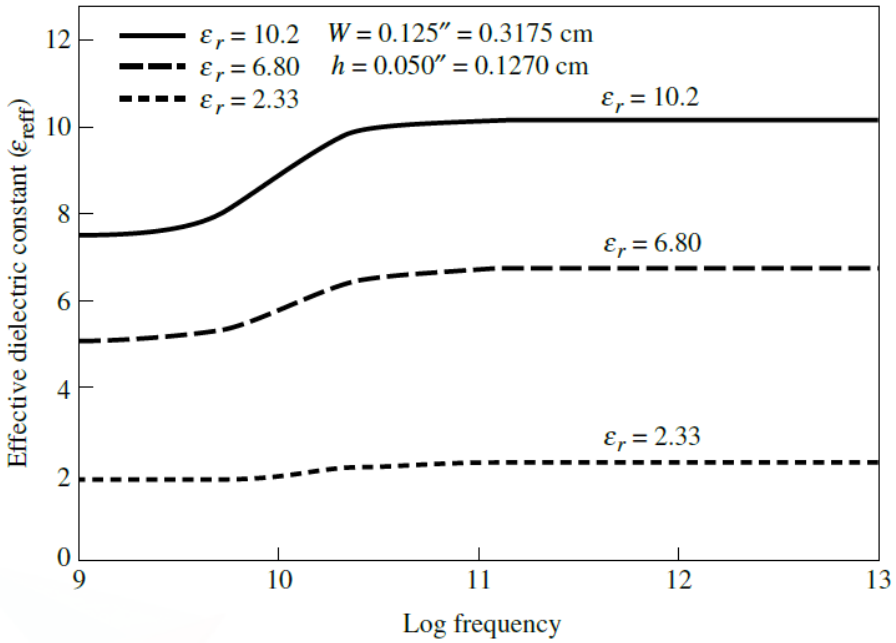

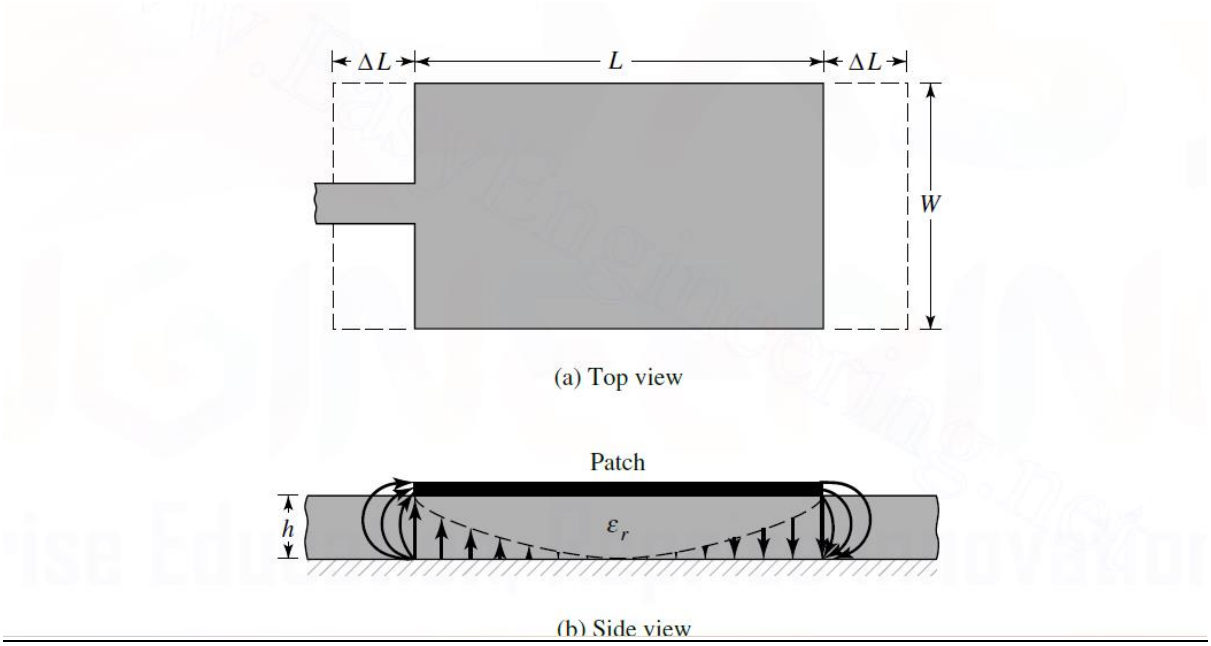

been extended on each end by a distance *L*, which is a function of the effective dielectric constant *I*reff and the width-to-height ratio (*W*/*h*). A very popular and practical

approximate relation for the normalized extension of the length is
L

$$\frac{\Delta L}{h} = 0.412 \frac{(\epsilon_{reff} + 0.3)\left(\frac{W}{h} + 0.264\right)}{(\epsilon_{reff} - 0.258)\left(\frac{W}{h} + 0.8\right)}$$

Since the length of the patch has been extended by L oneach side, the effective length of the patch is now ($L = \lambda/2$ for dominant TM010 mode with no fringing)
Leff = $L + 2L$
For the dominant TM010 mode, the resonant frequency of the microstrip antenna is a function of its length. Usually it is given by

$$(f_r)_{010} = \frac{1}{2L\sqrt{\epsilon_r}\sqrt{\mu_0\epsilon_0}} = \frac{\upsilon_0}{2L\sqrt{\epsilon_r}} \qquad (14\text{-}4)$$

where υ_0 is the speed of light in free space. Since (14-4) does not account for fringing, it must be modified to include edge effects and should be computed using

$$(f_{rc})_{010} = \frac{1}{2L_{\text{eff}}\sqrt{\epsilon_{\text{reff}}}\sqrt{\mu_0\epsilon_0}} = \frac{1}{2(L + 2\Delta L)\sqrt{\epsilon_{\text{reff}}}\sqrt{\mu_0\epsilon_0}}$$
$$= q\frac{1}{2L\sqrt{\epsilon_r}\sqrt{\mu_0\epsilon_0}} = q\frac{\upsilon_0}{2L\sqrt{\epsilon_r}} \qquad (14\text{-}5)$$

The q factor is referred to as the *fringe factor* (length reduction factor). As the substrate height increases, fringing also increases and leads to larger separations between the radiating edges and lower resonant frequencies.
C. Design
Based on the simplified formulation that has been described, a design procedure is outlined which leads to practical designs of rectangular microstrip antennas. The procedure assumes that the specified information includes the dielectric constant of the substrate *(Ir)*, the resonant frequency *(fr)*, and the height of the substrate h. The procedure is as follows:

Specify:

$$\epsilon_r,\ f_r \text{ (in Hz), and } h$$

Determine:

$$W, L$$

Design procedure:

1. For an efficient radiator, a practical width that leads to good radiation efficiencies is [15]

$$W = \frac{1}{2f_r\sqrt{\mu_0\epsilon_0}}\sqrt{\frac{2}{\epsilon_r+1}} = \frac{\upsilon_0}{2f_r}\sqrt{\frac{2}{\epsilon_r+1}} \tag{14-6}$$

where υ_0 is the free-space velocity of light.

where $\upsilon 0$ is the free-space velocity of light.

2. Determine the effective dielectric constant of the microstrip antenna using (14-1).
3. Once W is found using (14-6), determine the extension of the length $3L$ using (14-2).
4. The actual length of the patch can now be determined by solving (14-5) for L, or

$$L = \frac{1}{2f_r\sqrt{\epsilon_{\text{reff}}}\sqrt{\mu_0\epsilon_0}} - 2\Delta L$$

D. Conductance

Each radiating slot is represented by a parallel equivalent admittance Y (with conductance G and susceptance B). This is shown in Figure 9. The slots are labeled as

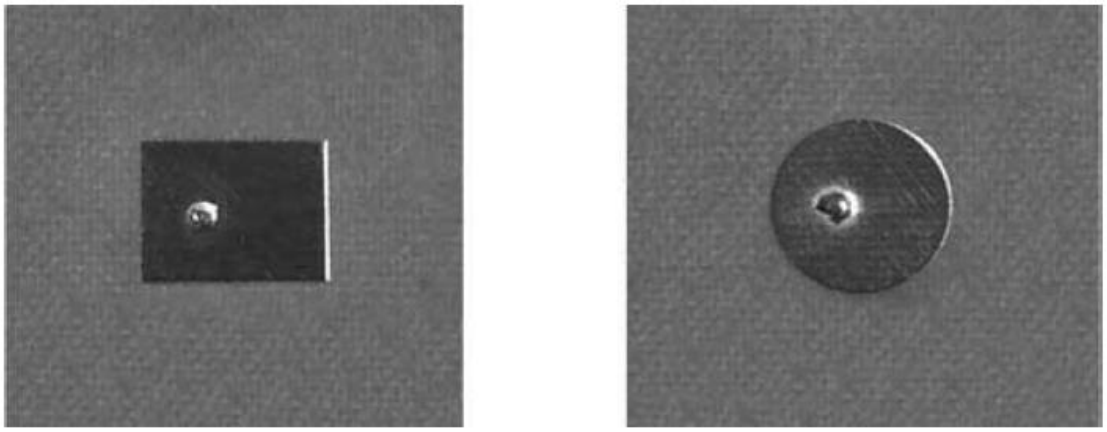

(a) rectangular (b) circular

#1 and #2. The equivalent admittance of slot #1, based on an infinitely wide, uniform slot, is derived in Example 12.8 of Chapter 12, and it is given by [81]

$Y1 = G1 + jB1$

where for a slot of finite width W

$$G_1 = \frac{W}{120\lambda_0}\left[1 - \frac{1}{24}(k_0 h)^2\right] \qquad \frac{h}{\lambda_0} < \frac{1}{10}$$

$$B_1 = \frac{W}{120\lambda_0}[1 - 0.636\ln(k_0 h)] \qquad \frac{h}{\lambda_0} < \frac{1}{10}$$

Since slot #2 is identical to slot #1, its equivalent admittance is

$$Y_2 = Y_1, \quad G_2 = G_1, \quad B_2 = B_1$$

The conductance of a single slot can also be obtained by using the field expression derived by the cavity model. In general, the conductance is defined as

$$G_1 = \frac{2P_{\text{rad}}}{|V_0|^2} \tag{14-10}$$

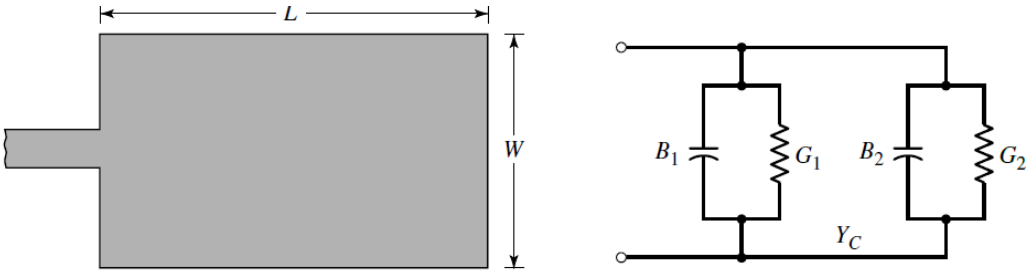

(a) Rectangular patch (b) Transmission model equivalent

Using the electric field of (14-41), the radiated power is written as

$$P_{\text{rad}} = \frac{|V_0|^2}{2\pi\eta_0}\int_0^{\pi}\left[\frac{\sin\left(\frac{k_0 W}{2}\cos\theta\right)}{\cos\theta}\right]^2 \sin^3\theta\, d\theta$$

Therefore the conductance of (14-10) can be expressed as

$$G_1 = \frac{I_1}{120\pi^2}$$

where

$$I_1 = \int_0^{\pi}\left[\frac{\sin\left(\frac{k_0 W}{2}\cos\theta\right)}{\cos\theta}\right]^2 \sin^3\theta\, d\theta$$

$$= -2 + \cos(X) + XS_i(X) + \frac{\sin(X)}{X}$$

$$X = k_0 W$$

Asymptotic values of (14-12) and (14-12a) are

$$G_1 = \begin{cases} \frac{1}{90}\left(\frac{W}{\lambda_0}\right)^2 & W \ll \lambda_0 \\ \frac{1}{120}\left(\frac{W}{\lambda_0}\right) & W \gg \lambda_0 \end{cases}$$

The values of (14-13) for $W \_ \lambda 0$ are identical to those given by (14-8a) for $h \_ \lambda 0$.

A plot of G as a function of $W/\lambda 0$ is shown in Figure 14.10.

E. Resonant Input Resistance

The total admittance at slot #1 (input admittance) is obtained by transferring the admittance of slot #2 from the output terminals to input terminals using the admittance transformation equation of transmission lines . Ideally the two slots should be separated by $\lambda/2$ where λ is the wavelength in the dielectric (substrate). However, because of fringing the length of the patch is electrically longer than the actual length. Therefore the actual separation of the two slots is slightly less than $\lambda/2$. If the reduction of the length is properly chosen using (14-2) (typically $0.48\lambda < L < 0.49\lambda$), the transformed admittance of slot #2 becomes

$$\tilde{Y}_2 = \tilde{G}_2 + j\tilde{B}_2 = G_1 - jB_1$$

$$\tilde{G}_2 = G_1$$

$$\tilde{B}_2 = -B_1$$

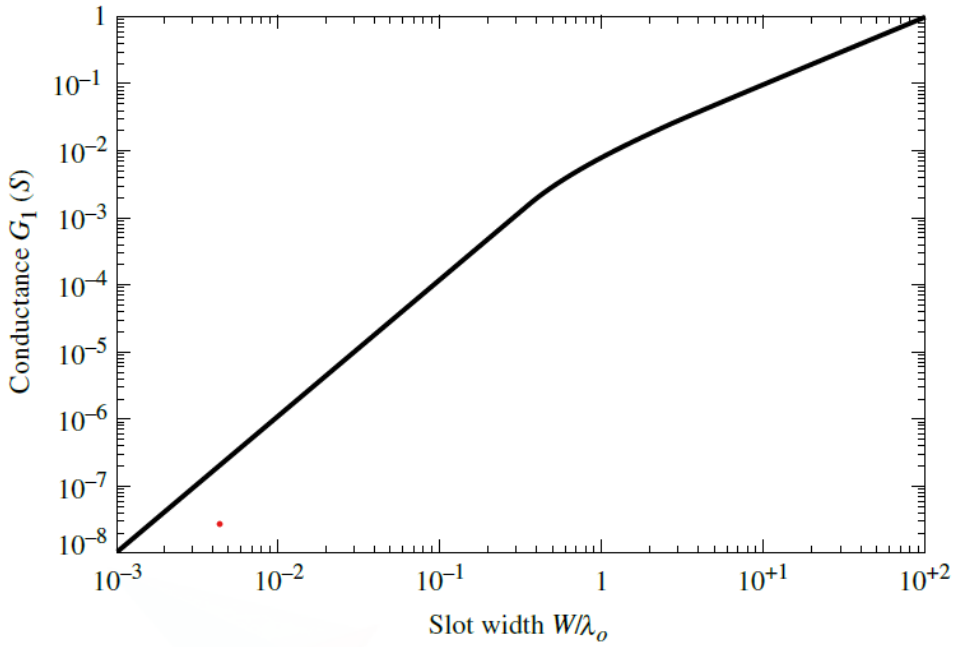

Therefore the total resonant input admittance is real and is given by

$$Y_{in} = Y_1 + \tilde{Y}_2 = 2G_1 \tag{14-15}$$

Since the total input admittance is real, the resonant input impedance is also real, or

$$Z_{in} = \frac{1}{Y_{in}} = R_{in} = \frac{1}{2G_1} \tag{14-16}$$

The resonant input resistance, as given by (14-16), does not take into account mutual effects between the slots. This can be accomplished by modifying (14-16) to [8]

$$R_{in} = \frac{1}{2(G_1 \pm G_{12})} \tag{14-17}$$

where the plus (+) sign is used for modes with odd (antisymmetric) resonant voltage distribution beneath the patch and between the slots while the minus (−) sign is used for modes with even (symmetric) resonant voltage distribution. The mutual conductance is defined, in terms of the far-zone fields, as

$$G_{12} = \frac{1}{|V_0|^2} \mathrm{Re} \iint_S \mathbf{E}_1 \times \mathbf{H}_2^* \cdot d\mathbf{s} \tag{14-18}$$

where $\mathbf{E}_1$ is the electric field radiated by slot #1, $\mathbf{H}_2$ is the magnetic field radiated by slot #2, V_0 is the voltage across the slot, and the integration is performed over a sphere of large radius. It can be shown that G_{12} can be calculated using [8], [34]

$$G_{12} = \frac{1}{120\pi^2} \int_0^{\pi} \left[\frac{\sin\left(\frac{k_0 W}{2} \cos\theta\right)}{\cos\theta} \right]^2 J_0(k_0 L \sin\theta) \sin^3\theta \, d\theta \tag{14-18a}$$

where $J0$ is the Bessel function of the first kind of order zero. For typical microstrip antennas, the mutual conductance obtained using (14-18a) is small compared to the self conductance $G1$ of (14-8a) or (14-12).

As shown by (14-8a) and (14-17), the input resistance is not strongly dependent Upon the substrate height h. Infact for very small values of h, such that $k0h$ _ 1, the input resistance is not dependent on h. Modal-expansion analysis also reveals that the input resistance is not strongly influenced by the substrate height h. It is apparent from (14-8a) and (14-17) that the resonant input resistance can be decreased by increasing the width W of the patch. This is acceptable as long as the ratio of W/L does not exceed 2 because the aperture efficiency of a single patch begins to drop, as W/L increases beyond 2.

The resonant input resistance, as calculated by (14-17), is referenced at slot #1. However, it has been shown that the resonant input resistance can be changed by using an inset feed, recessed a distance $y0$ from slot #1, as shown in Figure 11(a). This technique can be used effectively to match the patch antenna using a microstrip-line

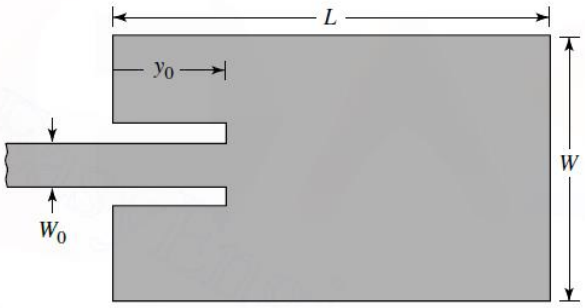

(a) Recessed microstrip-line feed

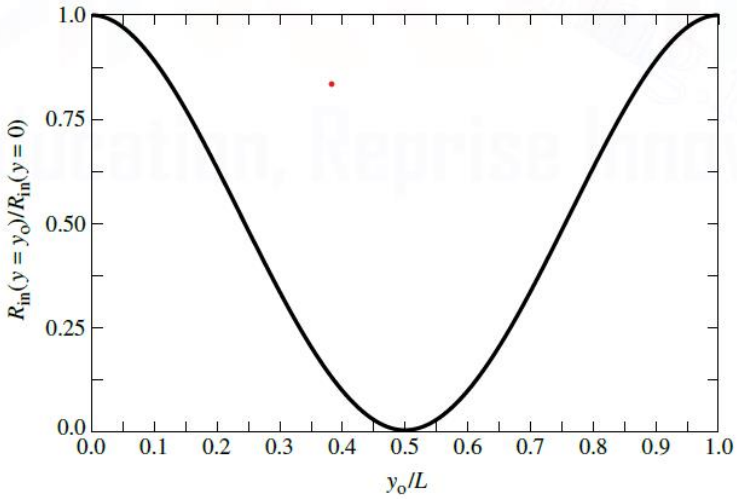

(b) Normalized input resistance

feed whose characteristic impedance is given by [79]

$$Z_c = \begin{cases} \dfrac{60}{\sqrt{\epsilon_{reff}}} \ln\left[\dfrac{8h}{W_0} + \dfrac{W_0}{4h}\right], & \dfrac{W_0}{h} \le 1 \quad (14\text{-}19a) \\ \dfrac{120\pi}{\sqrt{\epsilon_{reff}}\left[\dfrac{W_0}{h} + 1.393 + 0.667 \ln\left(\dfrac{W_0}{h} + 1.444\right)\right]}, & \dfrac{W_0}{h} > 1 \quad (14\text{-}19a) \end{cases}$$

where W_0 is the width of the microstrip line, as shown in Figure 14.11. Using modal-expansion analysis, the input resistance for the inset feed is given approximately by [8], [16]

$$R_{in}(y = y_0) = \frac{1}{2(G_1 \pm G_{12})}\left[\cos^2\left(\frac{\pi}{L}y_0\right) + \frac{G_1^2 + B_1^2}{Y_c^2}\sin^2\left(\frac{\pi}{L}y_0\right) - \frac{B_1}{Y_c}\sin\left(\frac{2\pi}{L}y_0\right)\right] \quad (14\text{-}20)$$

where $Y_c = 1/Z_c$. Since for most typical microstrips $G_1/Y_c \ll 1$ and $B_1/Y_c \ll 1$, (14-20) reduces to

$$R_{in}(y = y_0) = \frac{1}{2(G_1 \pm G_{12})}\cos^2\left(\frac{\pi}{L}y_0\right) = R_{in}(y = 0)\cos^2\left(\frac{\pi}{L}y_0\right) \quad (14\text{-}20a)$$

A plot of the normalized value of (14-20a) is shown in Figure 14.11(b).
The values obtained using (14-20) agree fairly well with experimental data. However, the inset feed introduces a physical notch, which in turn introduces a junction capacitance. The physical notch and its corresponding junction capacitance influence slightly the resonance frequency, which typically may vary by about 1%. It is apparent from (20a) and Figure 11(b) that the maximum value occurs at the edge of the slot $(y0 = 0)$ where the voltage is maximum and the current is minimum; typical values are in the 150–300 ohms. The minimum value (zero) occurs at the center of the patch $(y0 = L/2)$ where the voltage is zero and the current is maximum. As the inset feed point moves from the edge toward the center of the patch the resonant input impedance decreases monotonically and reaches zero at the center. When the value of the inset feed point approaches the center of the patch $(y0 = L/2)$, the $\cos 2(\pi y0/L)$ function varies very rapidly; therefore, the input resistance also changes rapidly with the position of the feed point. To maintain very accurate values, a close tolerance must be preserved.

2.CST(COMPUTER SIMULATION TECHNOLOGY)

CST Studio Suite is one of several software available in the SIMULIA software suite. SIMULIA makes virtual testing a standard business practice the improves product performance, reduces physical prototyping, and drives innovation. Unlike its competitors, CST Studio Suite is a complete technology using a single user interface to give access to multiple solvers, crucially including the robust and multifunctional Time Domain Solver, as detailed below.

What is CST Studio Suite Used For?

CST Studio Suite's electromagnetic and multi-physics solvers provide for a broad range of industry applications: from 5G MIMO antenna array design, to MRI and implant safety in life sciences. CST Studio Suite is vital to understanding the ways in which electromagnetic components will behave when your products are out in the real world – before you even consider costly, physical prototyping.

CST Studio Suite users have access to the most robust simulation solvers applying methods such as Time Domain Solver and Frequency Solver. CST Electromagnetic solvers are divided into disciplines: High Frequency, Low Frequency, Multiphysics, Particles, and EMC (Electromagnetic Compatibility) & EDA (Electronic Design Automation).

Which Solvers Are Included in CST Studio Suite?

CST Studio Suite includes a comprehensive range of electromagnetic and multiphysics solvers. Below you'll find a list of the most frequently used solvers, including their most common applications.

High Frequency

Time Domain

- Powerful and versatile 3D full-wave solver with both FIT (Finite Integration Technique) and TLM (Transition Line Matrix) implementations. Capable of performing broadband simulations in a single run. Suitable for extremely large, complex and detailed simulations.
- Applications include general high-frequency, transient effects, and 3D electronics.

Frequency Domain

- Powerful multi-purpose 3D full-wave solver based on the FEM (Finite Element Method). Capable of simulating many component types simultaneously and includes an MOR (Model-Order Reduction) feature for accelerating the simulation of resonant structures.
- Applications include general high-frequency simulation in small-to-medium sized models, resonant structures, multi-port systems and 3D electronics.

Hybrid Solver Task

- Enables linking of Time Domain, Frequency Domain, Integral Equation, and Asymptotic Solvers for hybrid simulation. Capable of processing projects with very wide frequency bands, or electrically large structures with very fine details. Includes bidirectional links between solvers for more accurate simulation.
- Applications include small antennas on very large structures, EMC simulation, and human body simulation in complex environments.

Asymptotic

- Ray-tracing solver based on the SBR (Shooting Bouncing Ray) method. Capable of handling simulations with an electric size of many thousands of wavelengths.
- Applications include electrically very large structures, installed performance of antennas scattering analysis.

Eigenmode

- 3D solver based on the AKS (Advanced Krylov Subspace) method and the JDM (Jacob-Davidson) method. For use with highly resonant filter structures, high-Q particle accelerator cavities and slow wave structures.

- Applications include filters, cavities, metamaterials and periodic structures.

Filter Designer 3D

- Synthesis tool for designing bandpass and diplexer filters which enables the realization of the 3D filter through Assembly Modeling.
- Applications include cross-coupled filters for various electromagnetic technologies, and assistive tuning for filter hardware.

Integral Equation

- 3D full-wave solver based on the MOM (Methods of Movement) technique with MLFMM (Multilevel Fast Multipole Method). Capable of simulating large models with lots of empty space highly efficiently and includes a CMA (Characteristic Mode Analysis) feature which calculates the modes supported by a structure.
- Applications include electrically large models, installed performance, and characteristic mode analysis.

Multilayer

- 3D full-wave solver based on the MOM (Methods of Movement) technique. Capable of simulating planar microwave structures.
- Applications include MMIC, feeding networks and planar antennas.

Low Frequency

Electrostatic

- 3D Solver for simulating static electronic fields. Suitable for applications where electric charge of capacitance is important.
- Applications include sensors and touchscreens, power equipment, charged particle devices, and x-ray tubes.

Stationary Current

- 3D Solver for simulating the flow of DC currents through a device. Especially with lossy components.
- Applications include high-power equipment, electrical machines, and PCB power distribution networks.

Magnetostatic

- 3D Solver for simulating static magnetic fields. Capable of simulating magnets, sensors and electrical machines where the transient effects and eddy currents are not critical.
- Applications include sensors, motors, generators, and particle beam focusing magnets.

Low Frequency – Frequency Domain

- 3D Solver for simulating time-harmonic behavior in low frequency systems. Capable of performing in MQS (Magneto-Quasistatic), EQS (Electro-Quasistatic) and Fullwave implementations.

- Applications include sensors and NDS (Non-Destructive Testing), RFID and wireless power transfer, and power engineering.

Low Frequency – Time Domain

- 3D Solver for simulating transient behavior in low frequency systems. Capable of performing in MQS (Magneto-Quasistatic) and EQS (Electro-Quasistatic) implementations.
- Applications include electrical machines and transformers, electromechanical, and power engineering.

Multiphysics

Thermal Steady State Solver

- Capable of predicting temperature distribution in a steady-state system and the resulting impact on electromagnetic performance. Links seamlessly with electromagnetic solvers.
- Applications include high-power electronics components and devices, medical devices and bio-heating.

Thermal Transient Solver

- Capable of predicting time-varying temperature response of a system and the resulting impact on electromagnetic performance.
- Applications include high-power electronics components and devices, medical devices and bio-heating.

Conjugate Heat Transfer Solver

- Capable of predicting fluid flow and temperature distribution in a system using CFD (Computation Fluid Dynamics).
- Applications include electronics cooling.

Mechanical Solver

- Capable of predicting mechanical stress and deformation of structures caused by electromagnetic forces and thermal expression. Design for use with EM and Thermal solvers.
- Applications include filter detuning, PCB deformation, and Lorentz forces on particle accelerators.

Particles

Particle-in-Cell

- Particle tracking simulation method for calculating both trajectory and electromagnetic fields in the time-domain.
- Applications include accelerator components, slow-wave devices, and multipaction.

Particle Tracking

- 3D Solver for simulating particle trajectories through electromagnetic fields. Includes several emission models: fixed, space charge limited, thermionic, and field emission.
- Applications include particle sources, focusing and beam steering magnets, and accelerator components.

Wakefield

- The Wakefield solver is used for calculating fields around a particle beam.
- Applications include cavities, collimators, and beam position monitors.

EMC & EDA

PCB Solvers

- PCBs and Packages module for SI (Signal Integrity), PI (Power Integrity), and EMC (Electromagnetic Compatibility) analysis on PCBs (Printed Circuit Boards).
- Integrates easily with EDA design flow using popular layout tools from Cadence, Zuken, and Altium.
- CST Studio Suite includes three solver types for PCB Solvers:
    - 2D Transmission Line method
    - 3D PEEC (Partial Element Equivalent Circuit)
    - 3D FEFD (Finite-Element Frequency-Domain)
- Applications include high-speed PCBs, packages, and power electronics.

Rule Check

- EMC, (Electromagnetic Compatibility), SI (Signal Integrity), and PI (Power Integrity) design rule checking tool for automating EMC and SI design rule examination.
- Applications include EMC, SI and PI design rule checking.

Cable Harness Solver

- 3D analysis of SI (Signal Integrity), CE (Conducted Emission), RE (Radiated Emission), and EMS (Electromagnetic Susceptibility of complex cable structures in electrically large systems.
- Applications include general SI (Systems Integrity) and EMC (Electromagnetic Compatibility), cable harness layout in vehicles and aircraft, and hybrid cables in consumer electronics.

3. DESIGNING OF MICROSTRIP PATCH ANTENNA

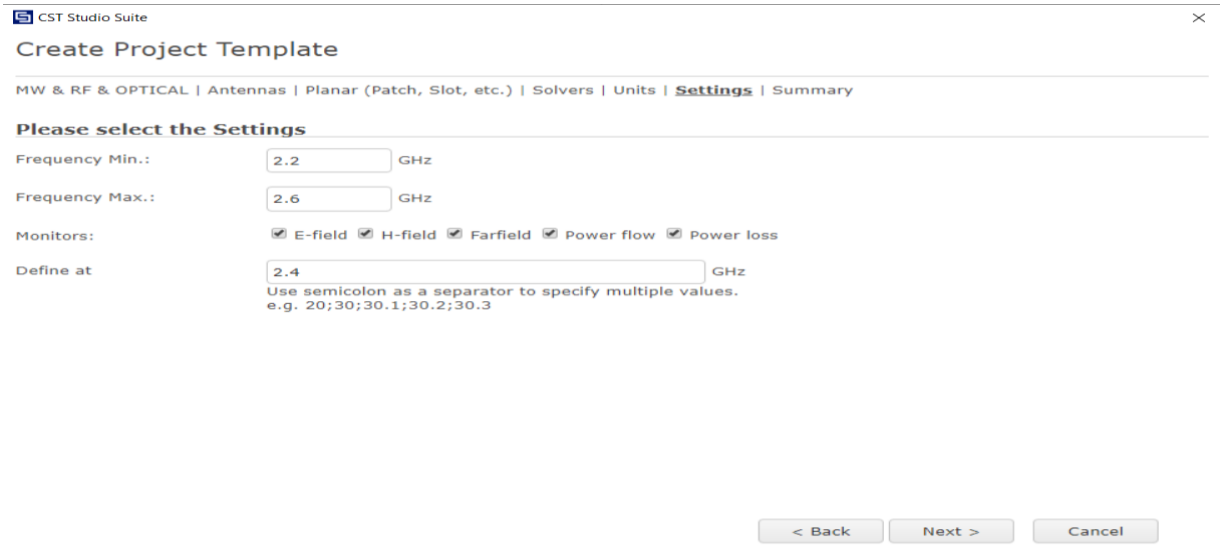

Setting up the minimum and maximum frequency for a microstrip patch antenna 2.2GHz and 2.6GHz are the min. and max. frequencies at which this antenna will operate. Resonant frequency is choosed at 2.4GHz.

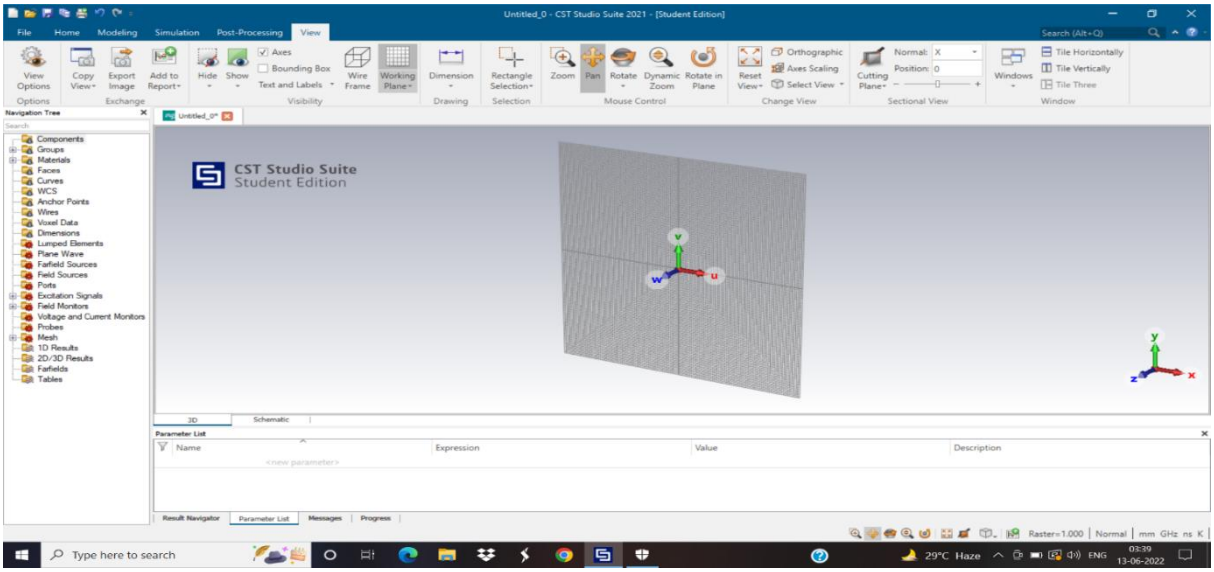

The above figure represents the represents the working plane of CST Studio Suite.

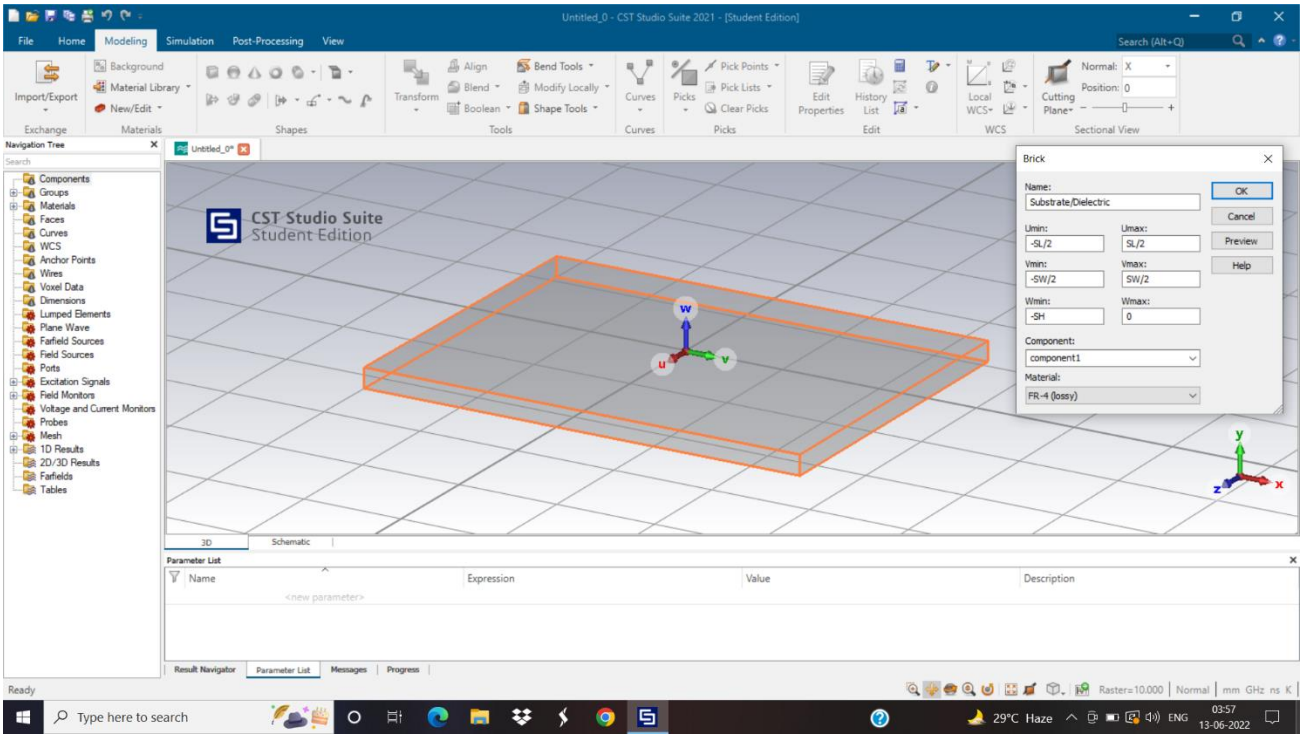

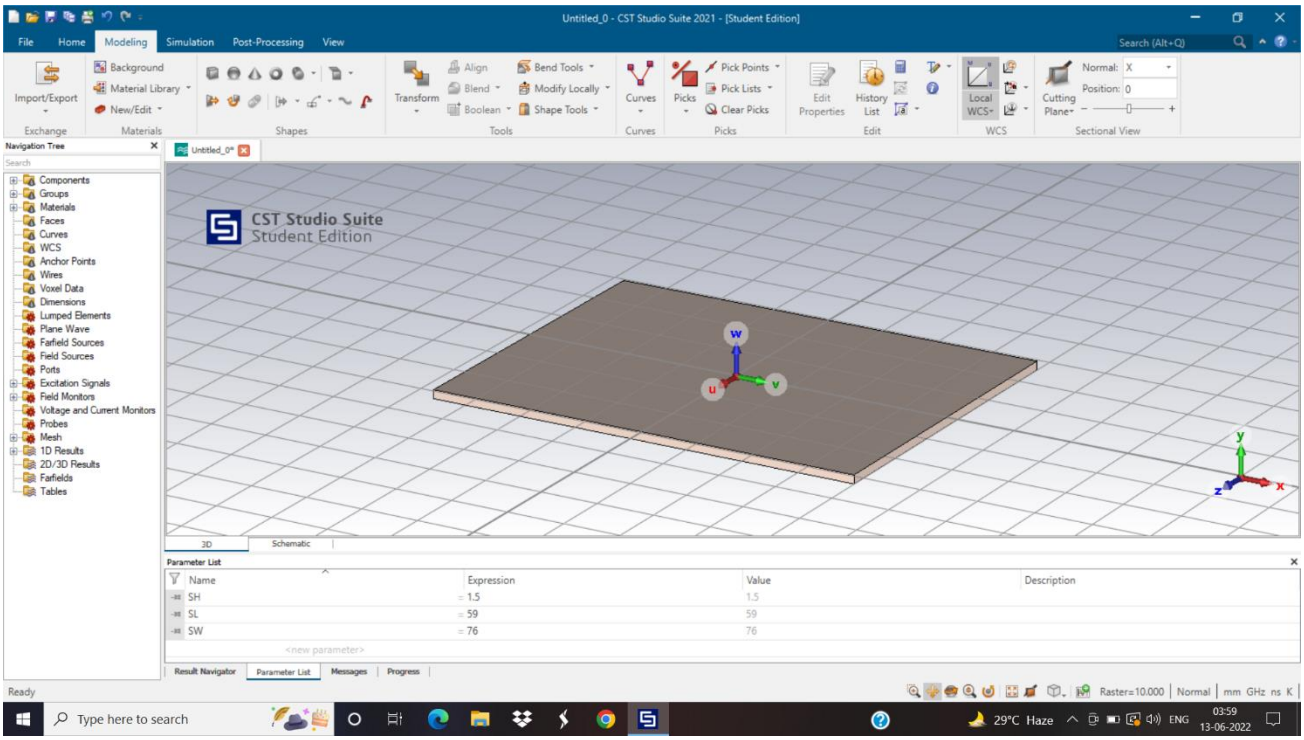

Designing of the substrate of MPA. Here the substrate used is FR-4(lossy) material with epsilon (relative permittivity)=4.3.

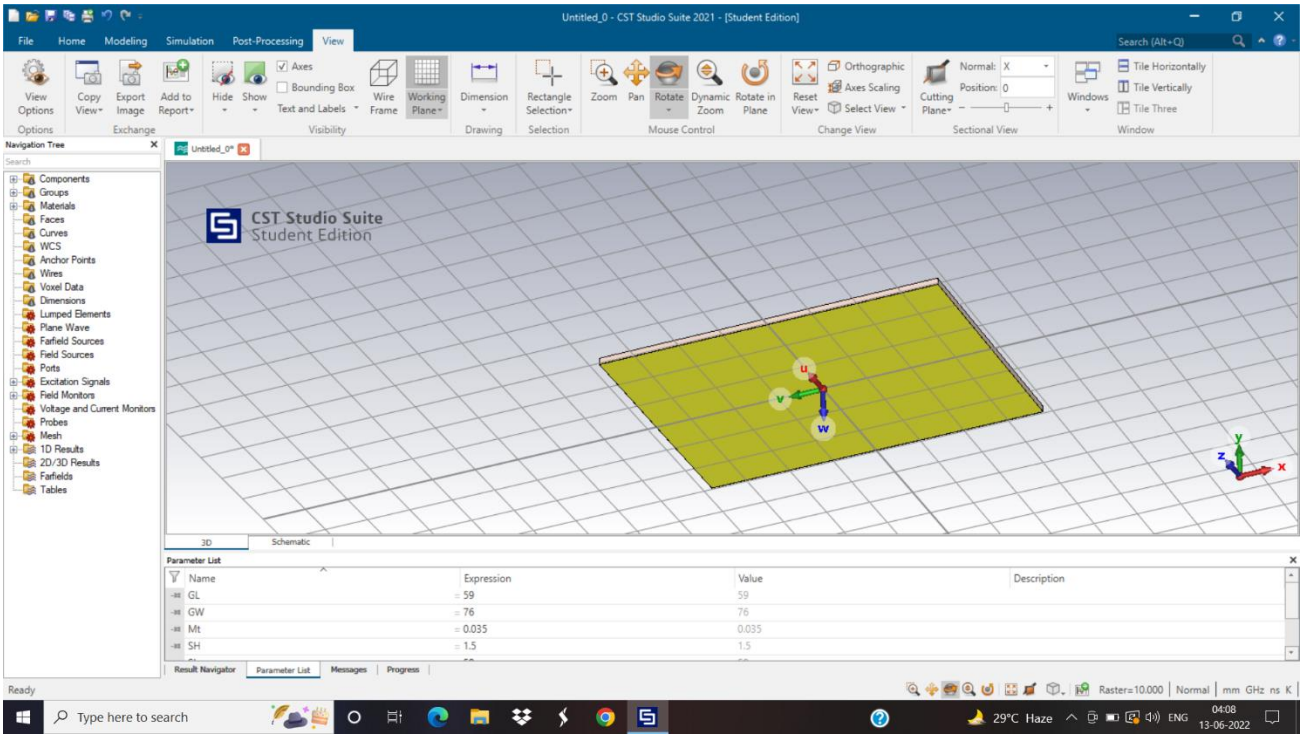

The above figure represents the designing of the ground plane of microstrip patch antenna.

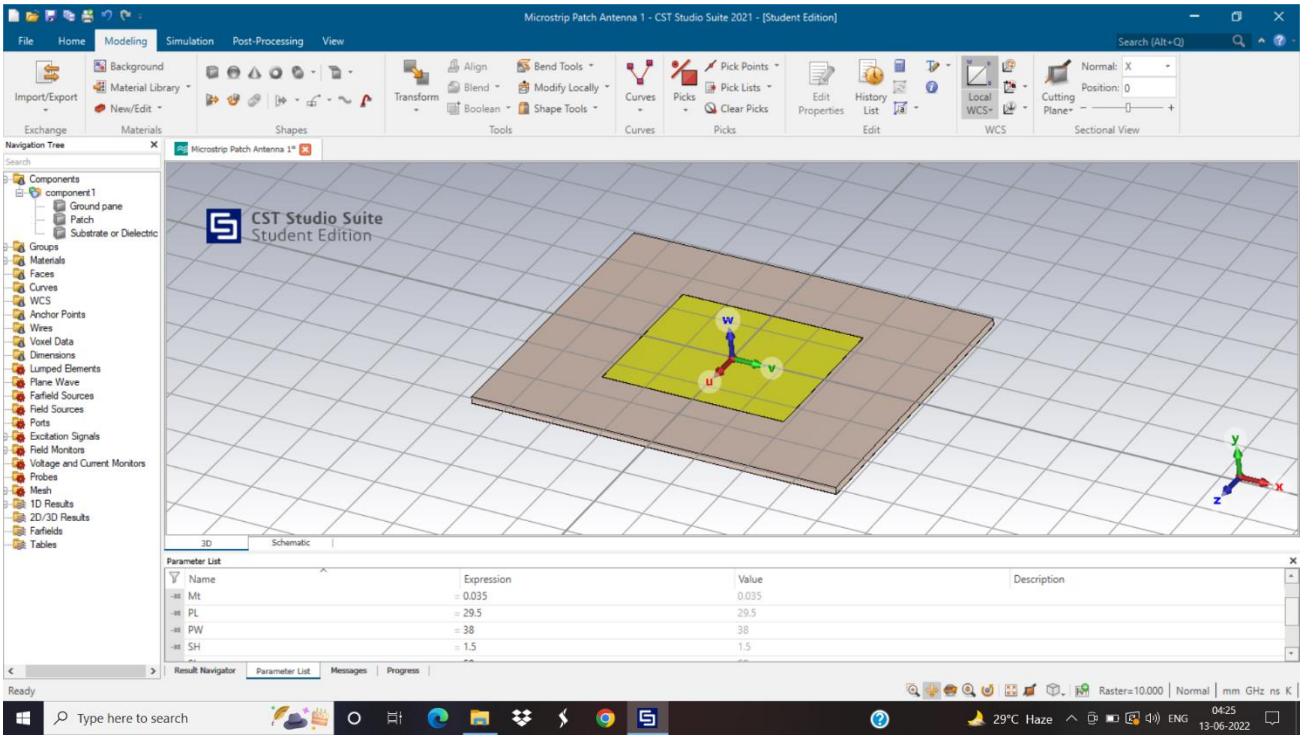

The above figure represents the designing of metallic patch above the dielectric material.

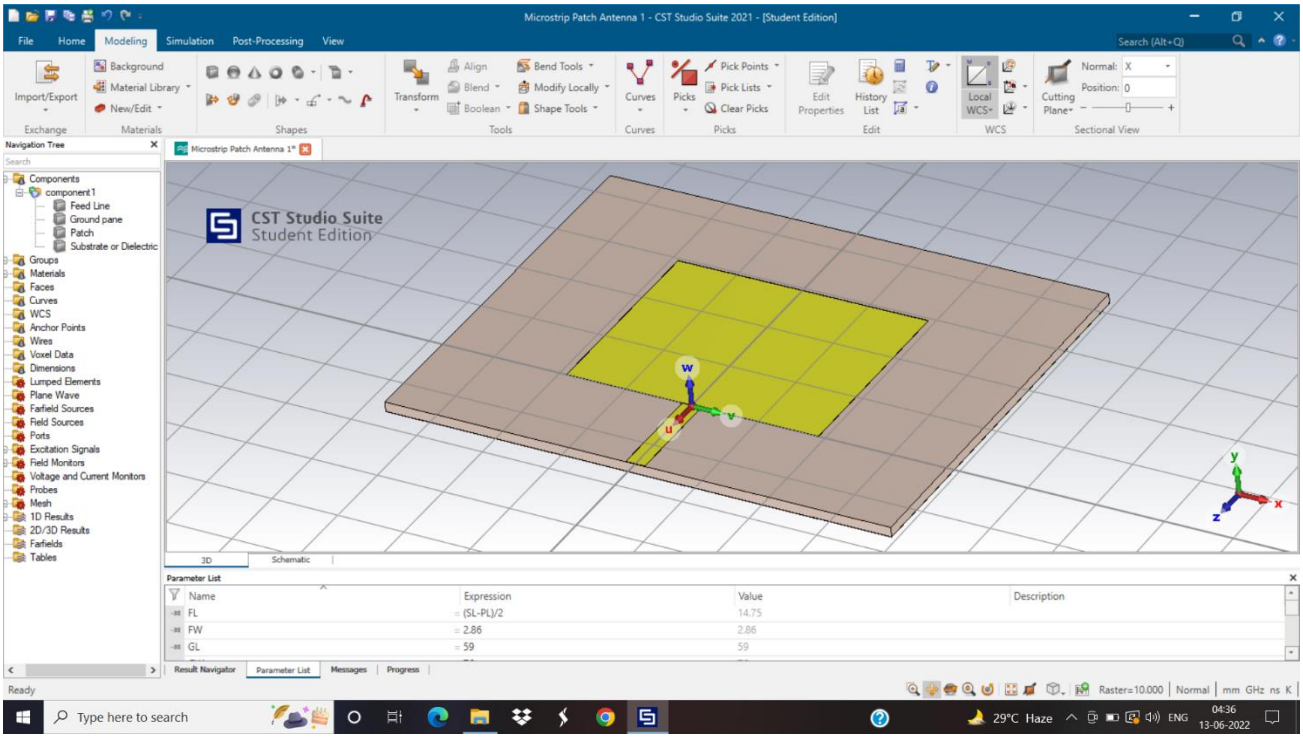

The above figure represents the designing of the field line of Microstrip patch antenna.

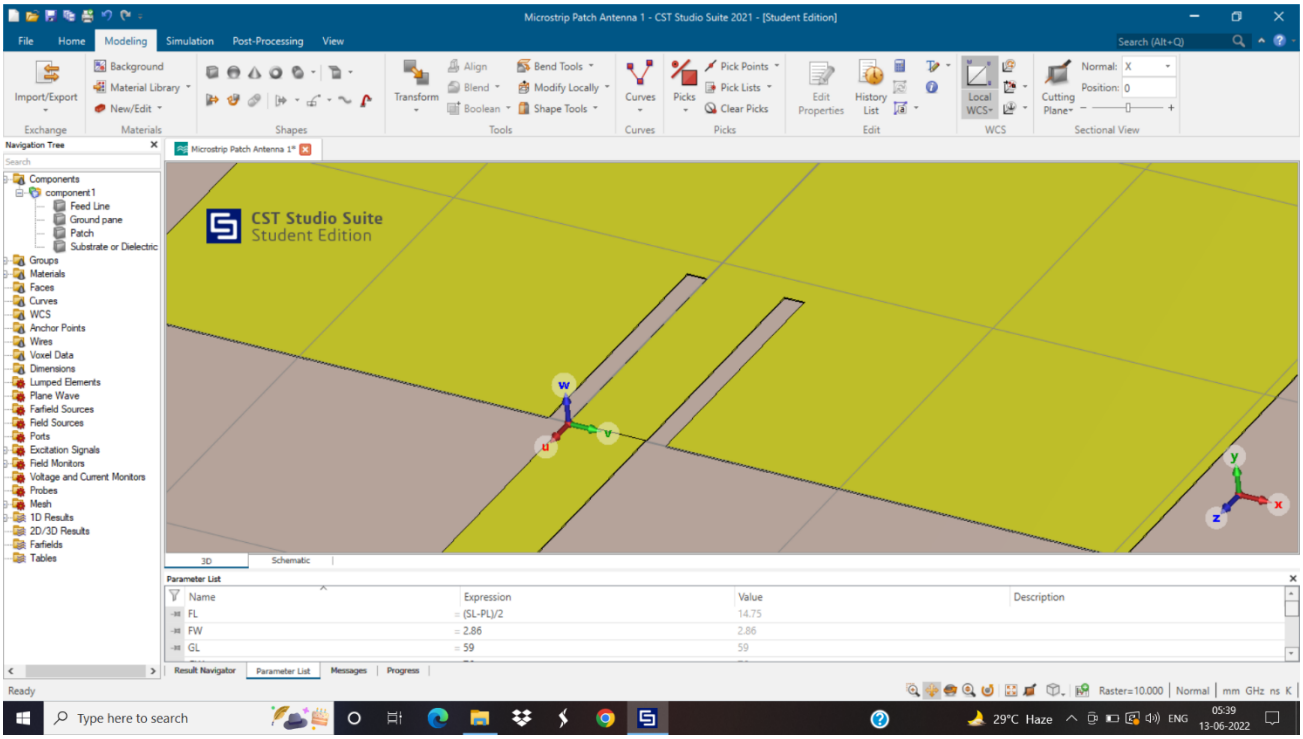

In this figure Inset is introduced in metallic patch in order to provide impedance matching.

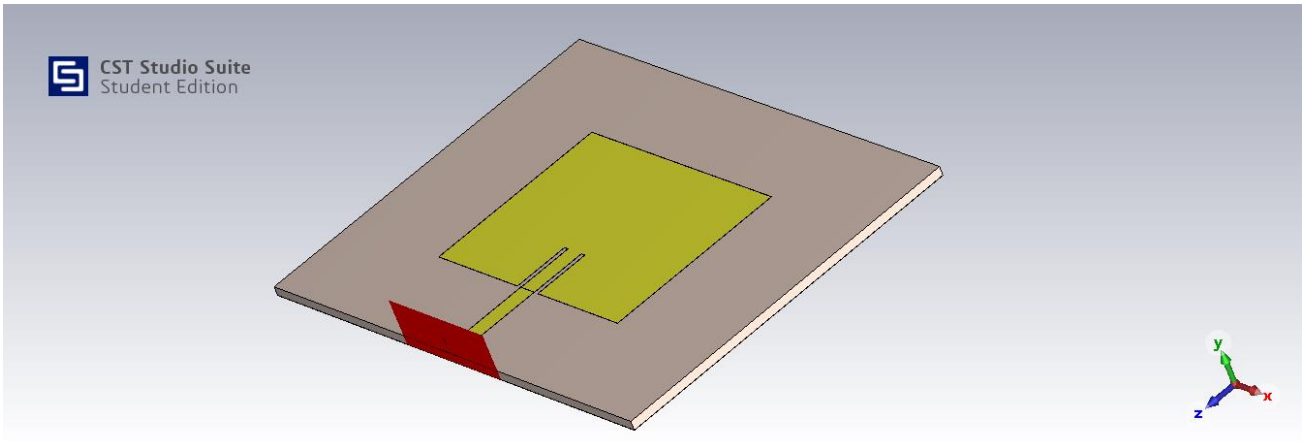

Fig: Final design of Microstrip Patch Antenna

The above figure represents the final design of Microstrip patch antenna.

4.SIMULATION REULTS/OBSERVATIONS

1D RESULTS:

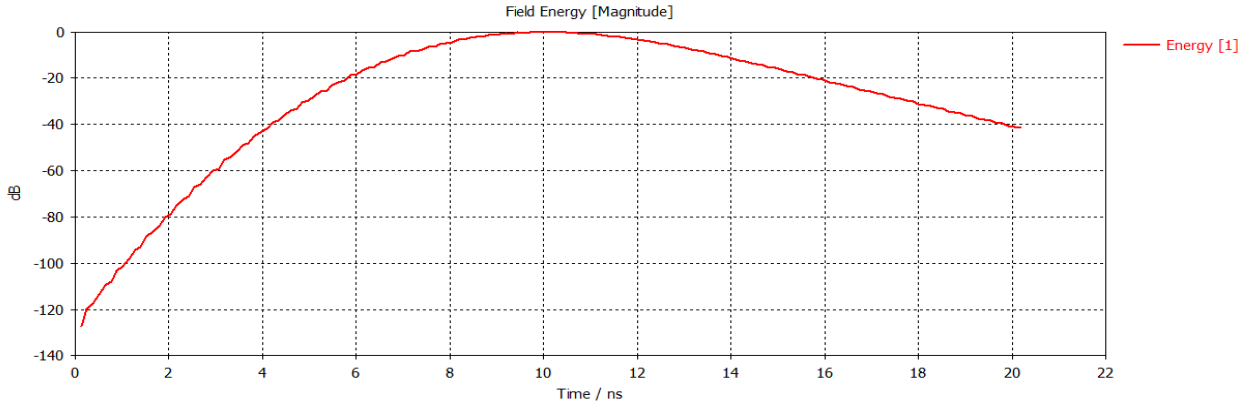

Fig: Field Energy

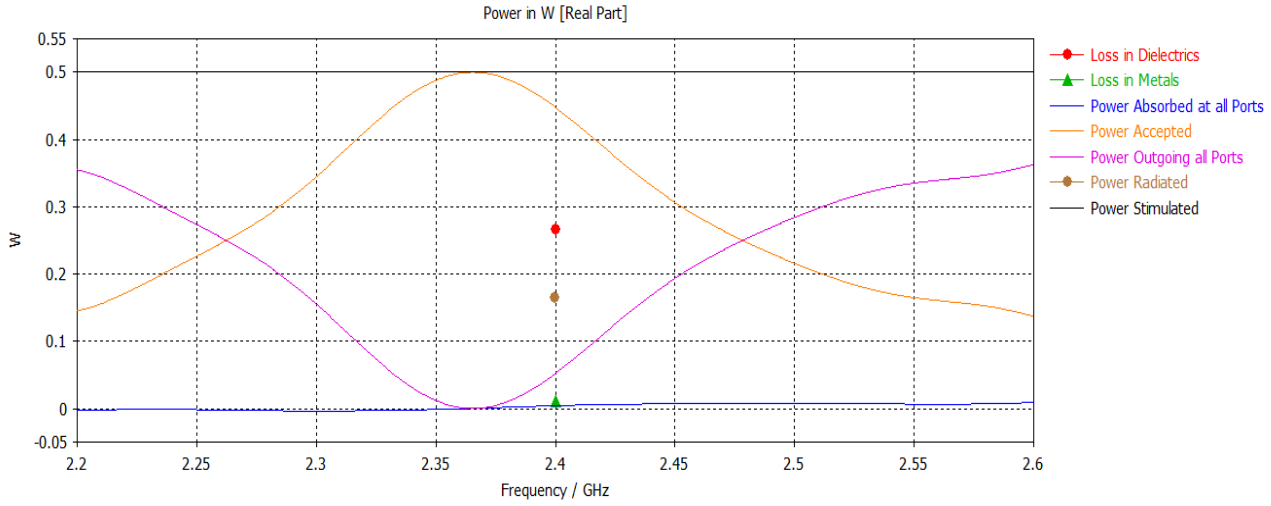

Fig: Power Distribution

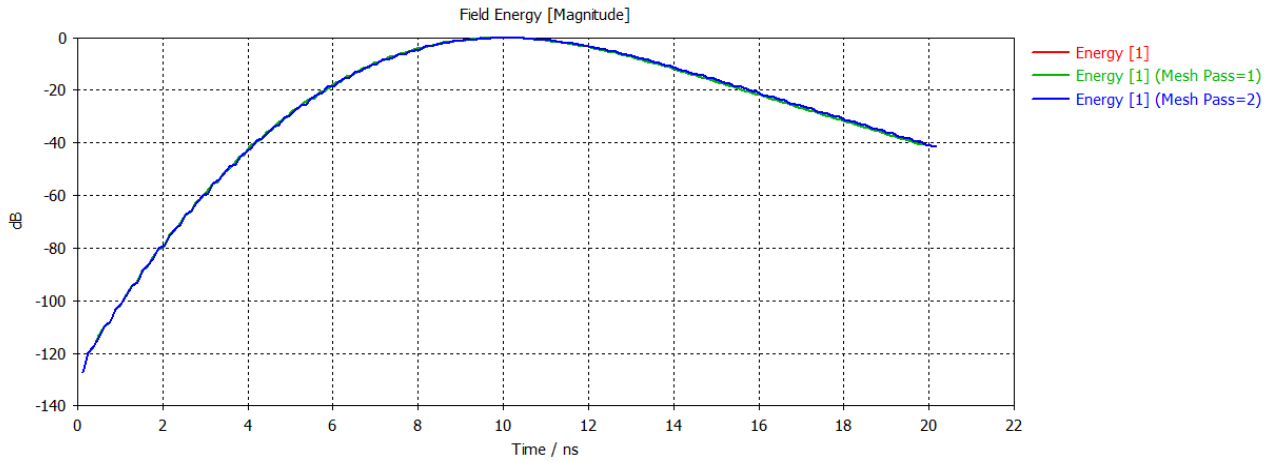
Field Energy [Magnitude]
dB
0
-20
-40
-60
-80
-100
-120
-140
0
2
4
6
8
10
12
14
16
18
20
22
Time / ns
Energy [1]
Energy [1] (Mesh Pass=1)
Energy [1] (Mesh Pass=2)

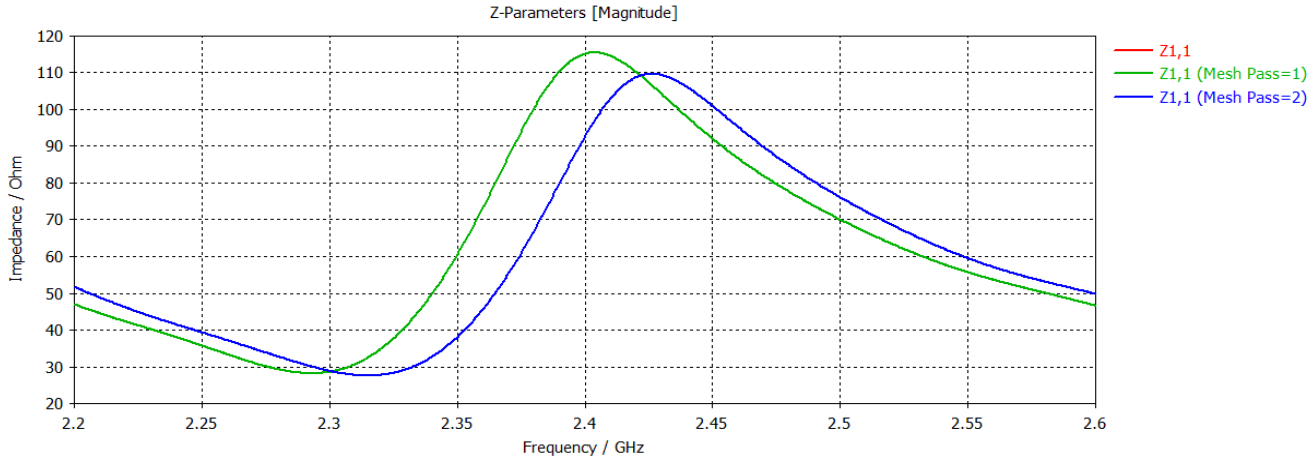
Z-Parameters [Magnitude]
Impedance / Ohm
120
110
100
90
80
70
60
50
40
30
20
2.2
2.25
2.3
2.35
2.4
2.45
2.5
2.55
2.6
Frequency / GHz
Z1,1
Z1,1 (Mesh Pass=1)
Z1,1 (Mesh Pass=2)

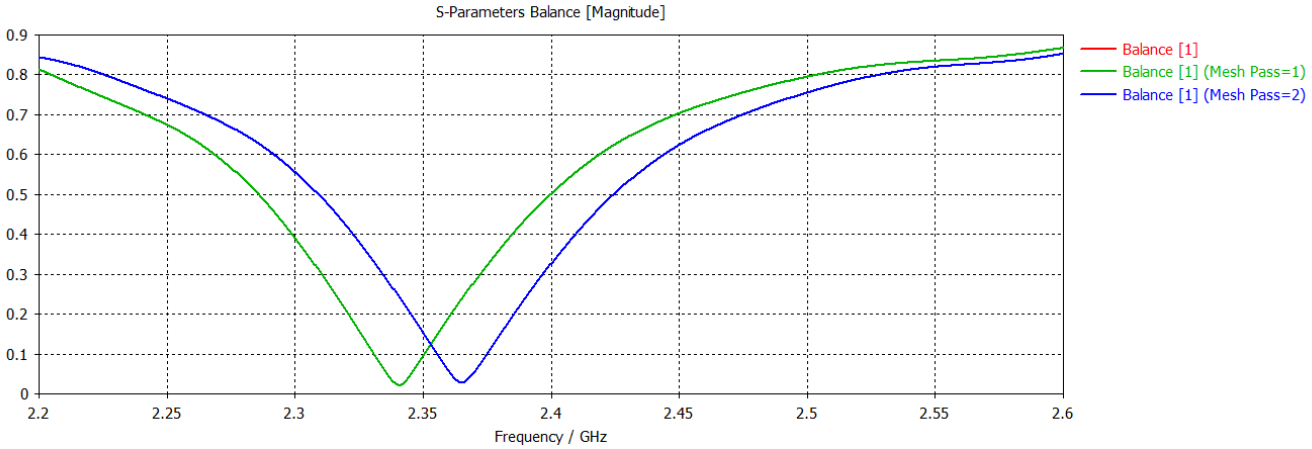
S-Parameters Balance [Magnitude]
0.9
0.8
0.7
0.6
0.5
0.4
0.3
0.2
0.1
0
2.2
2.25
2.3
2.35
2.4
2.45
2.5
2.55
2.6
Frequency / GHz
Balance [1]
Balance [1] (Mesh Pass=1)
Balance [1] (Mesh Pass=2)

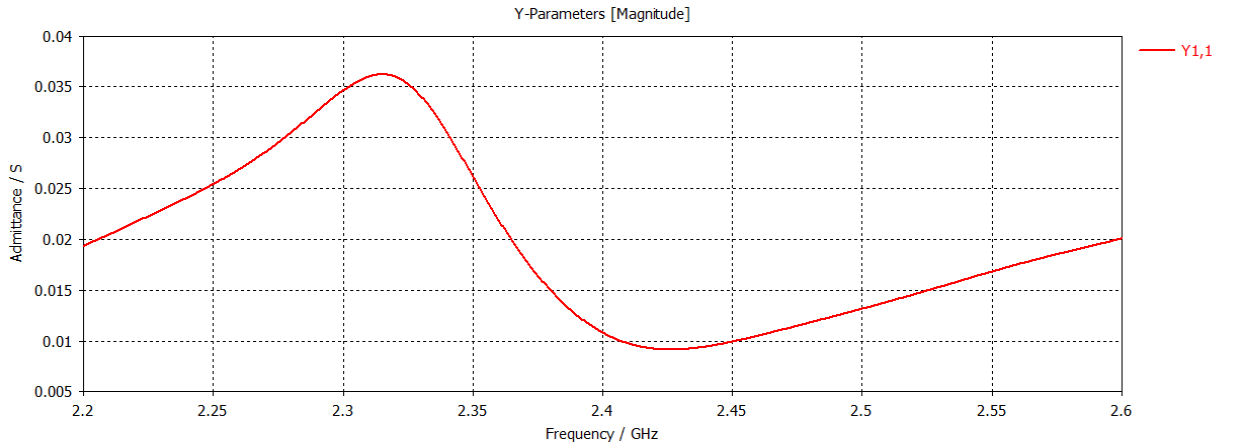
Y-Parameters [Magnitude]
Admittance / S
0.04
0.035
0.03
0.025
0.02
0.015
0.01
0.005
2.2
2.25
2.3
2.35
2.4
2.45
2.5
2.55
2.6
Frequency / GHz
Y1,1

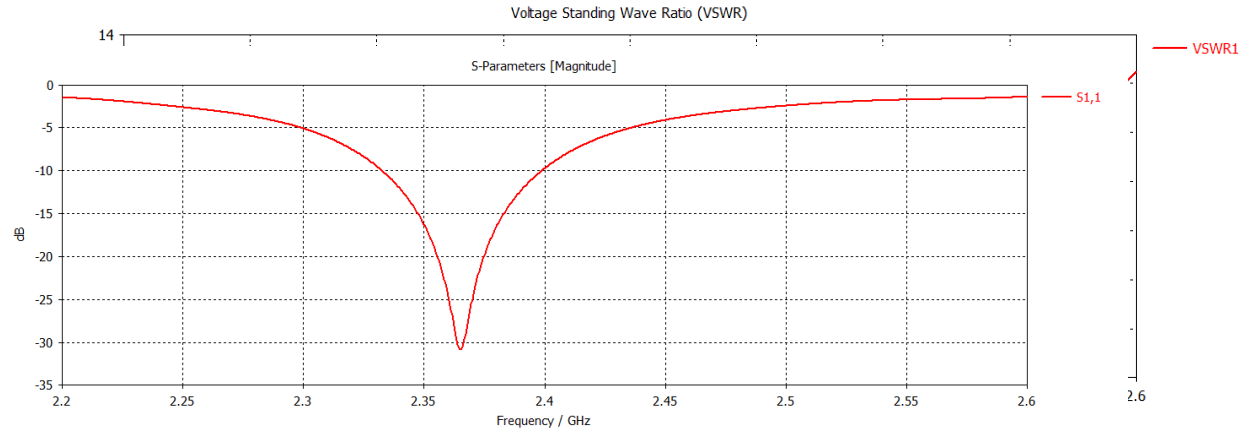
Voltage Standing Wave Ratio (VSWR)
14
S-Parameters [Magnitude]
dB
0
-5
-10
-15
-20
-25
-30
-35
2.2
2.25
2.3
2.35
2.4
2.45
2.5
2.55
2.6
Frequency / GHz
S1,1
VSWR1

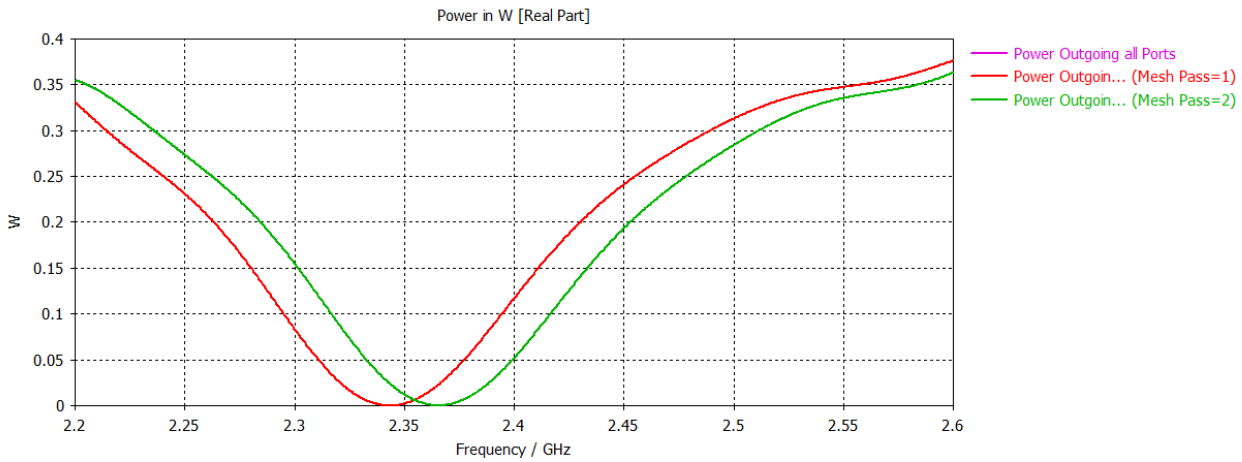
Power in W [Real Part]
W
0.4
0.35
0.3
0.25
0.2
0.15
0.1
0.05
0
2.2
2.25
2.3
2.35
2.4
2.45
2.5
2.55
2.6
Frequency / GHz
Power Outgoing all Ports
Power Outgoin... (Mesh Pass=1)
Power Outgoin... (Mesh Pass=2)

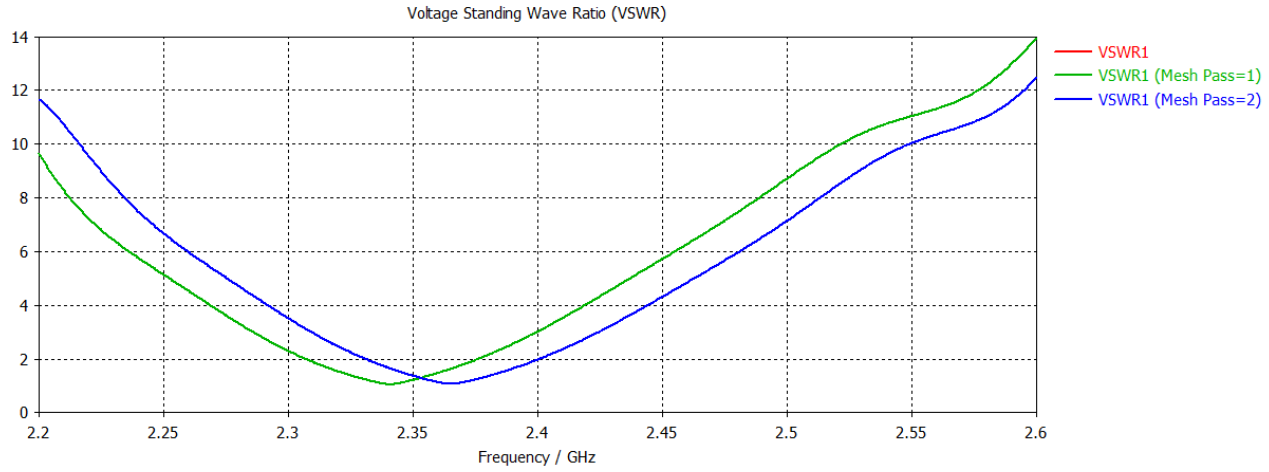

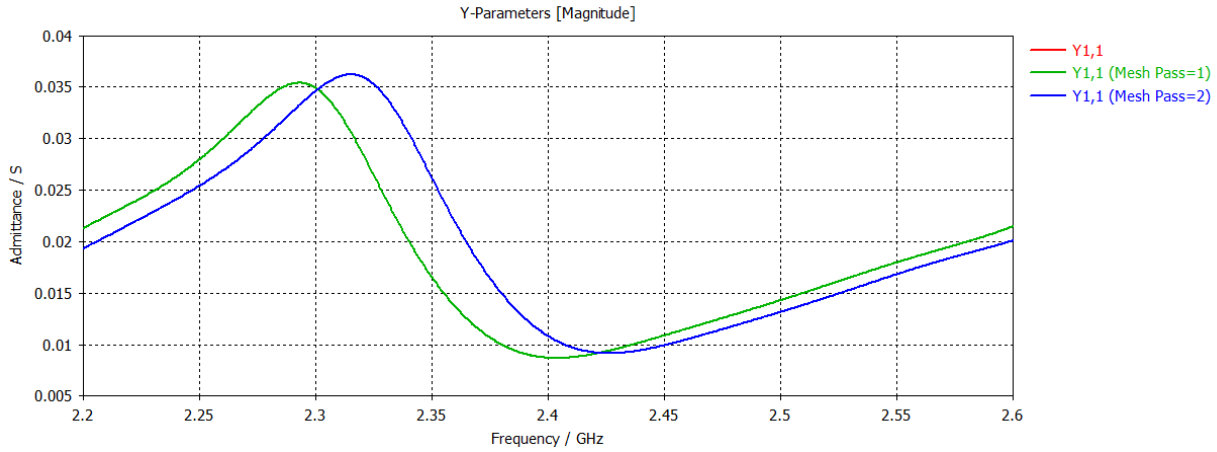

Fig: Y parameter (for separate mesh pass)

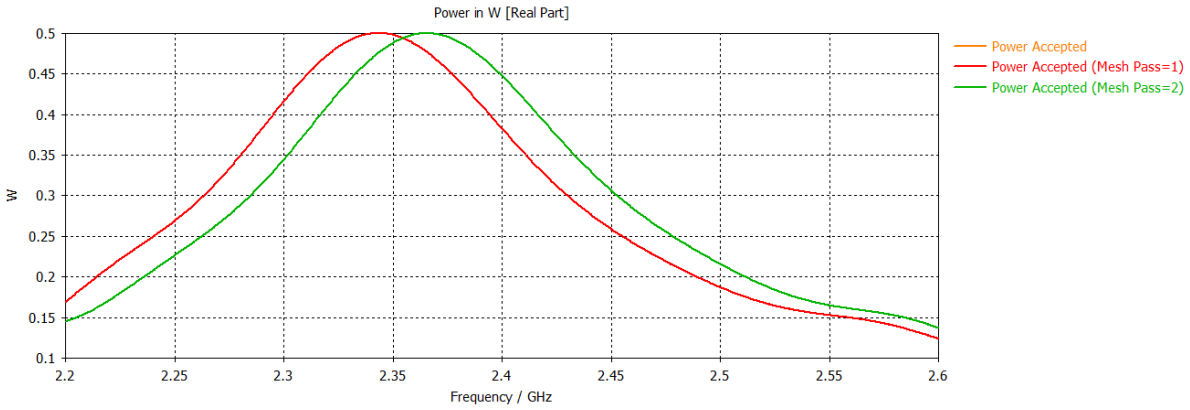

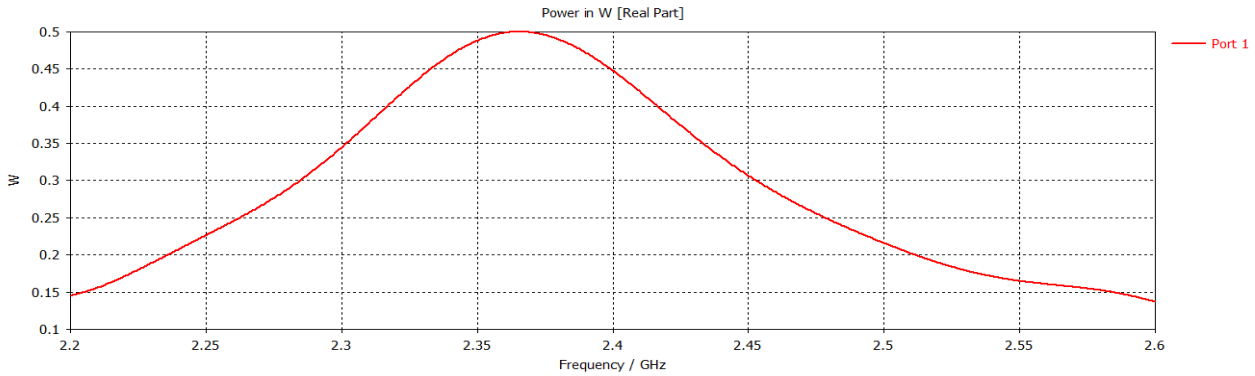
Power in W [Real Part]
W
Frequency / GHz
Port 1

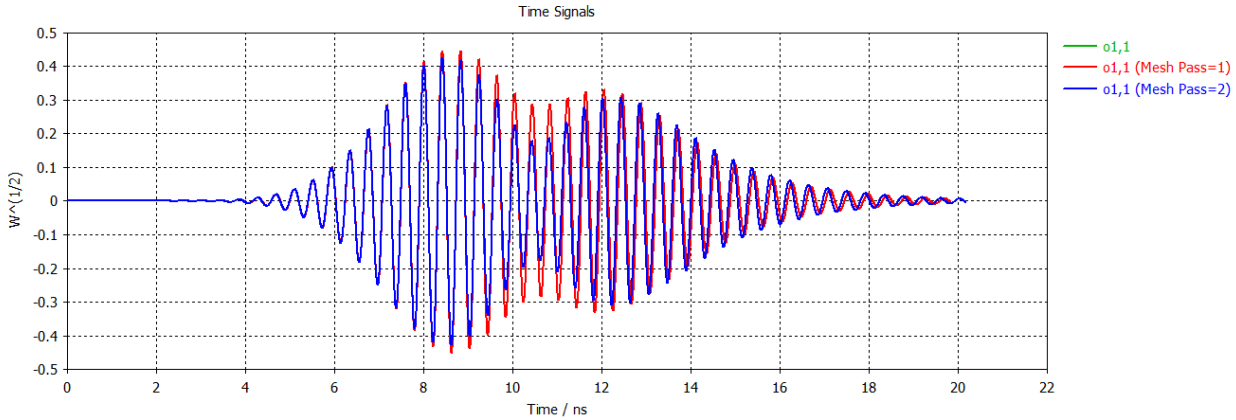
Time Signals
W^(1/2)
Time / ns
o1,1
o1,1 (Mesh Pass=1)
o1,1 (Mesh Pass=2)

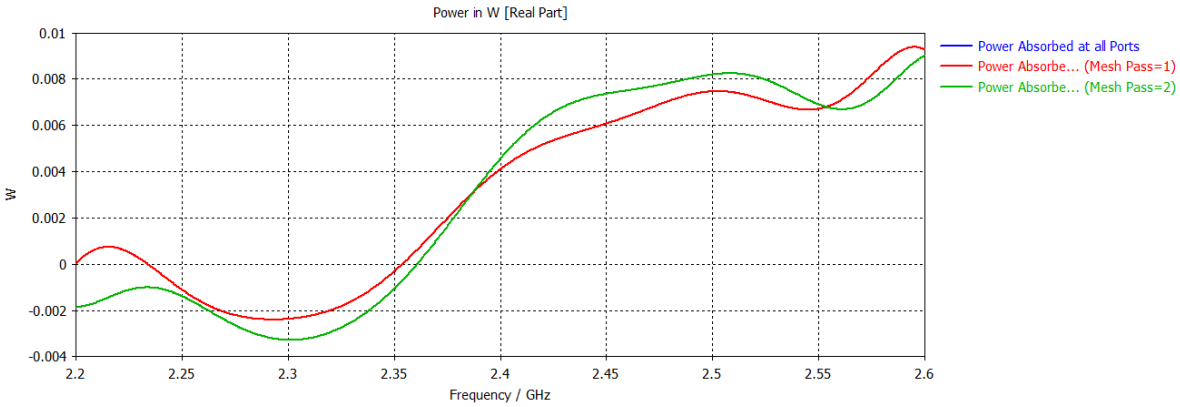
Power in W [Real Part]
W
Frequency / GHz
Power Absorbed at all Ports
Power Absorbe... (Mesh Pass=1)
Power Absorbe... (Mesh Pass=2)

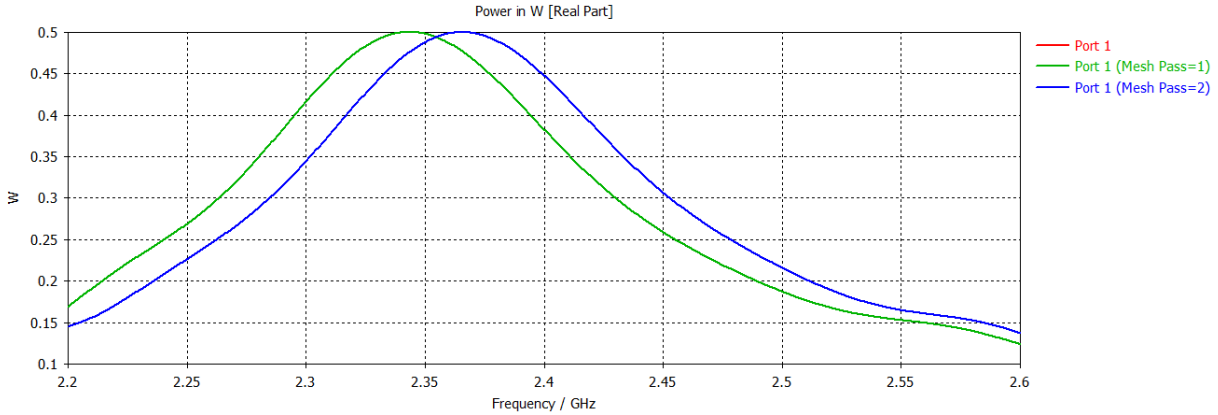
Power in W [Real Part]
W
Frequency / GHz
Port 1
Port 1 (Mesh Pass=1)
Port 1 (Mesh Pass=2)

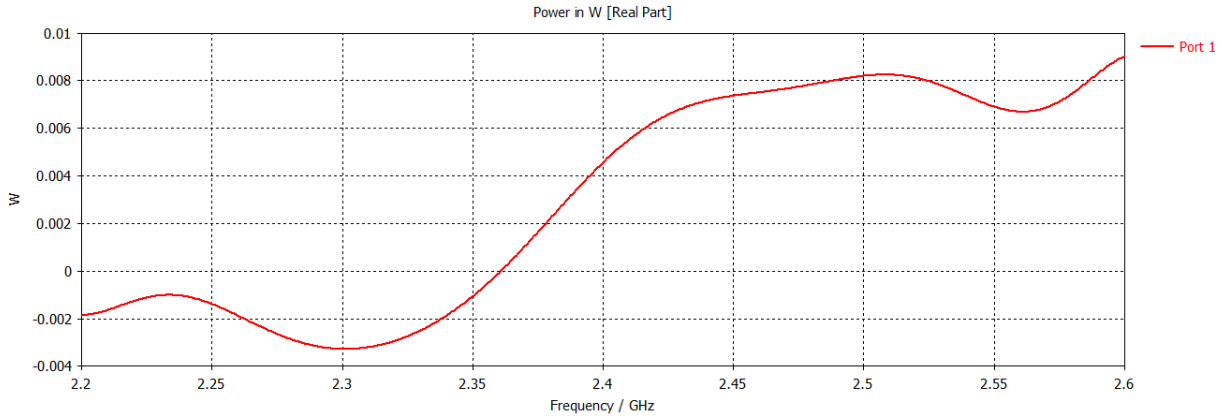

Fig: Power in watts

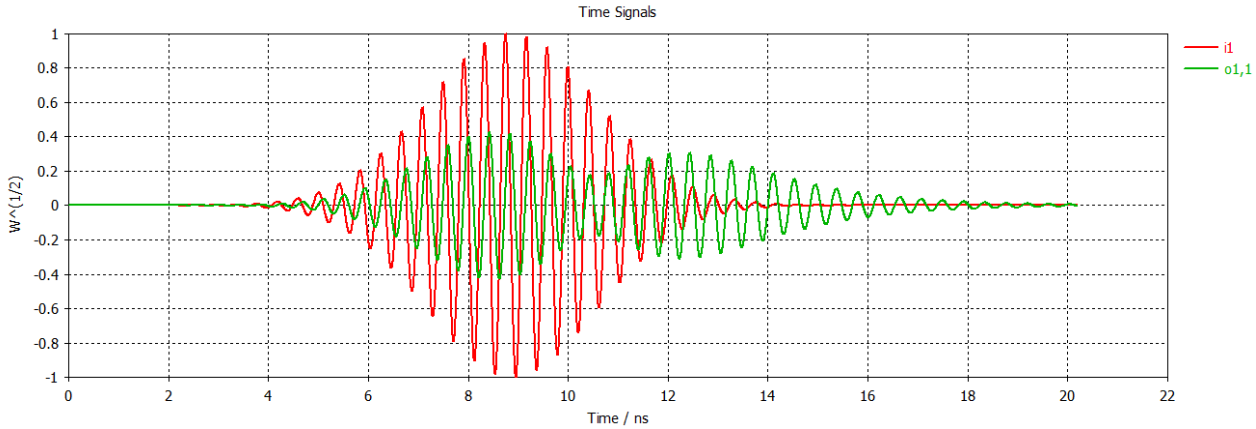

Fig: Time signals

2D RESULTS:

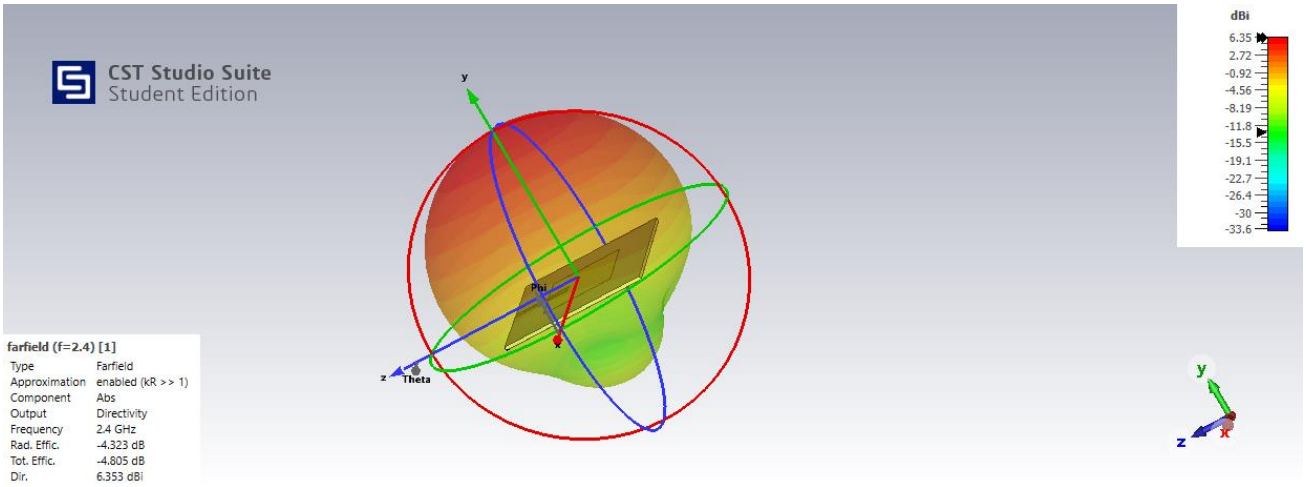

Fig: Directivity 3D

Directivity of an antenna is defined as the ratio of the radiation intensity in a given direction from the antenna to the radiation intensity averaged over all directions. Here, the final design of microstrip patch antenna has directivity of 6.353 dBi. The average radiation intensity is equal to the total power radiated by the antenna divided by 4π. If the direction is not strictly specified, the direction of maximum radiation intensity is implied. Directivity is a measure of how well the array directs energy toward a particular direction. The directivity is independent of the scan angle and for a uniformly illuminated linear array $D = 2L_x/\lambda$, where L_x is the length of the linear array; this is the maximum directivity obtained by a linear array.

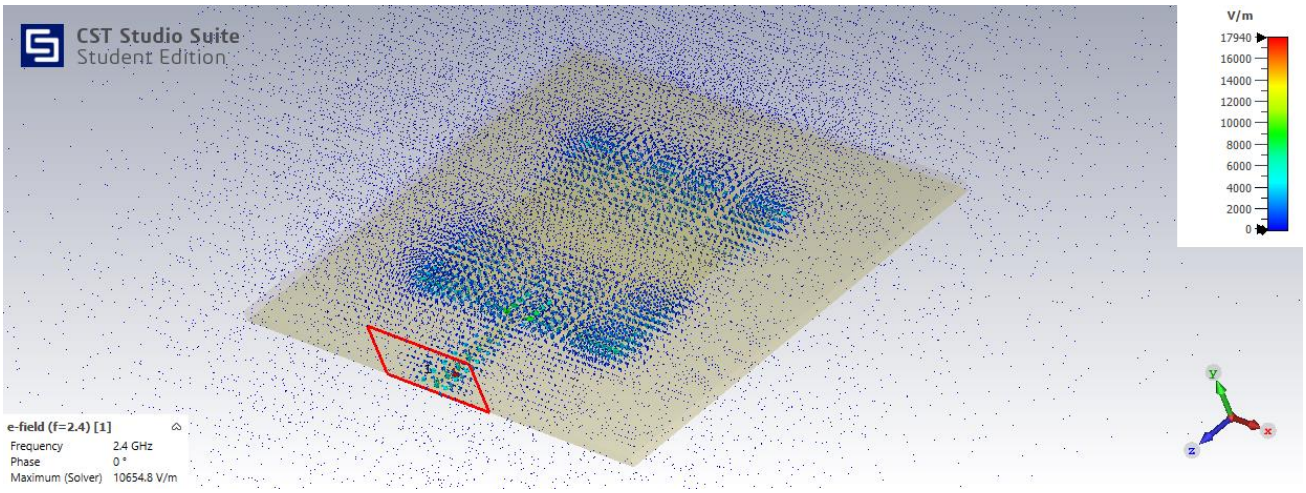

The above figure shows how magnetic field is distributed in the outer periphery of patch antenna.

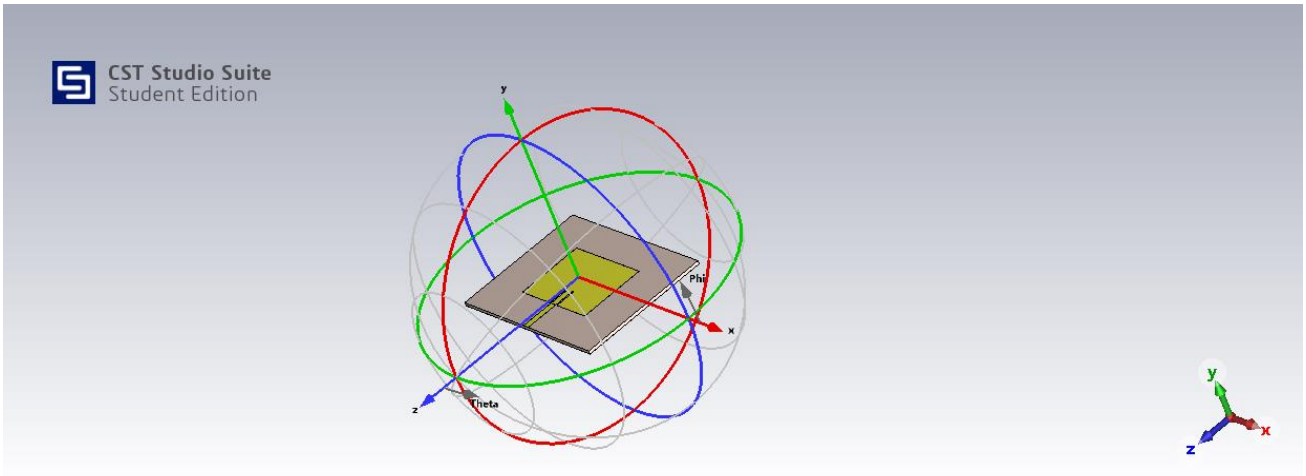

Fig: Far field cuts 3D

The above figure gives the idea of farfield of microstrip patch antenna. The near field and far field are regions of the electromagnetic field around an object, such as a transmitting antenna, or the result of radiation scattering off an object. Non-radiative *near-field* behaviors dominate close to the antenna or scattering object, while electromagnetic radiation *far-field* behaviors dominate at greater distances. Far-field E (electric) and B (magnetic) field strength decreases as the distance from the source increases, resulting in an inverse-square law for the radiated *power* intensity of electromagnetic radiation.

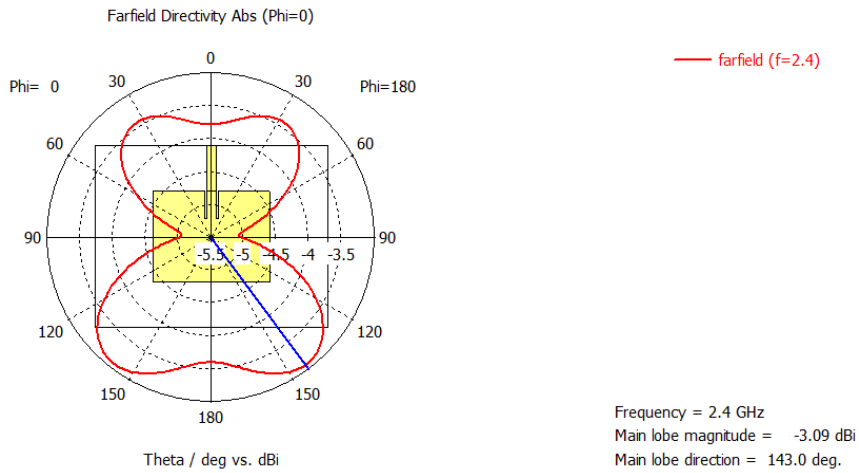

Fig: Far field cuts excitation at Phi=0^0

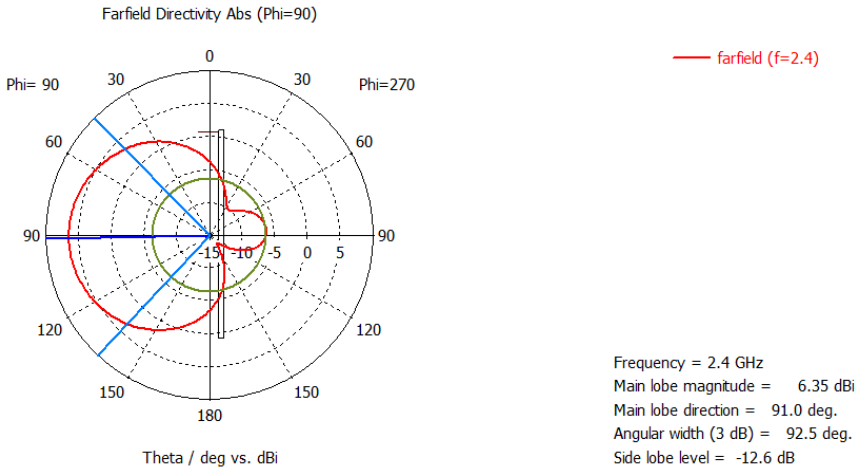

Fig: Far field cuts excitation at Phi=90^0

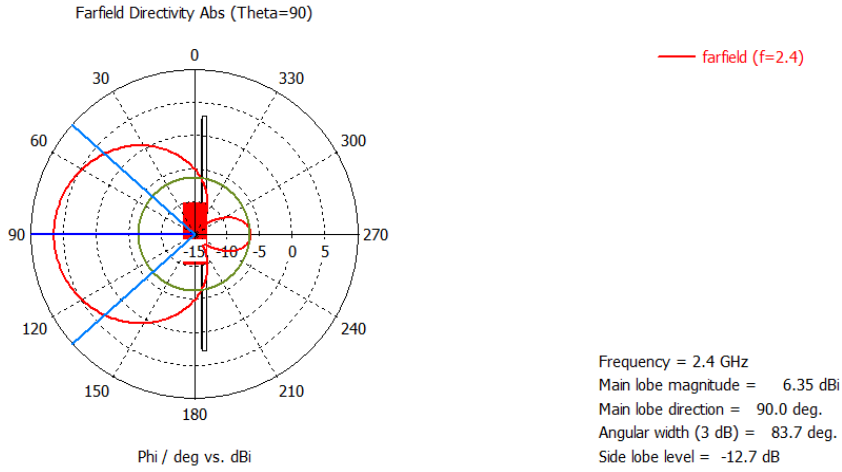

Fig: Far field cuts excitation at Theta=90^0

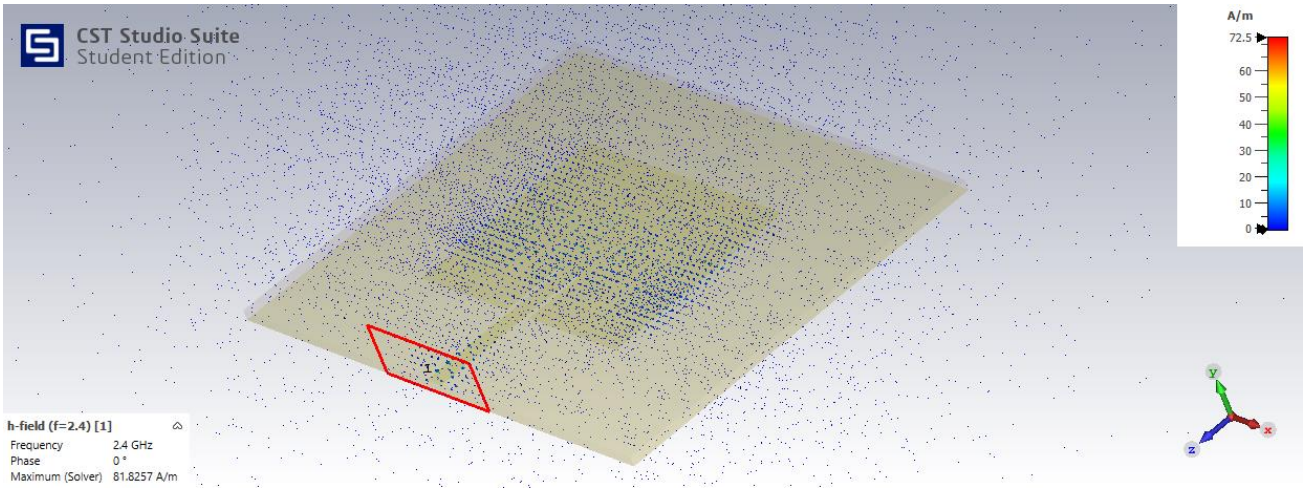

Fig: h-field (f=2.4)

The above figure shows how magnetic field is distributed around the microstrip patch antenna.

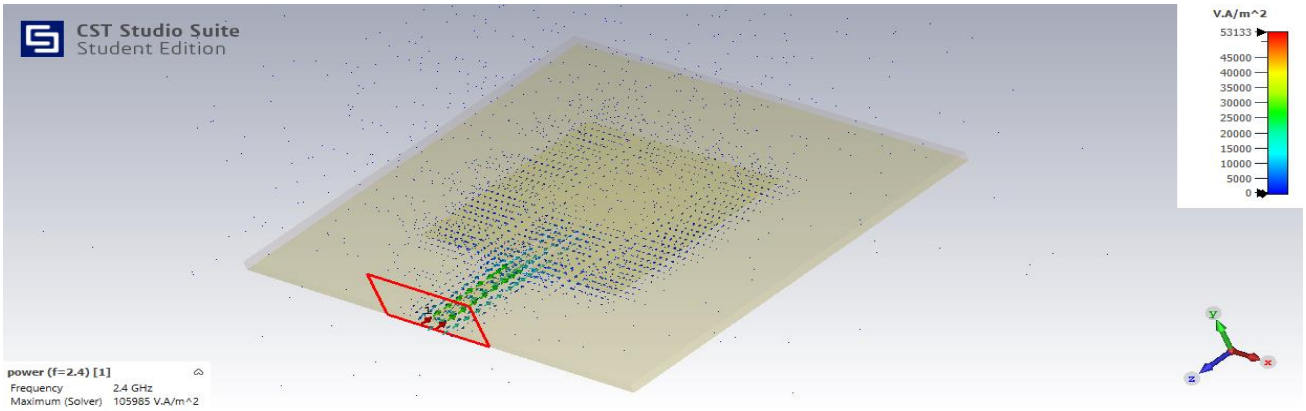

Fig: Power flow in microstrip patch antenna(f=2.4)

The above figure shows how power flows in microstrip patch antenna.

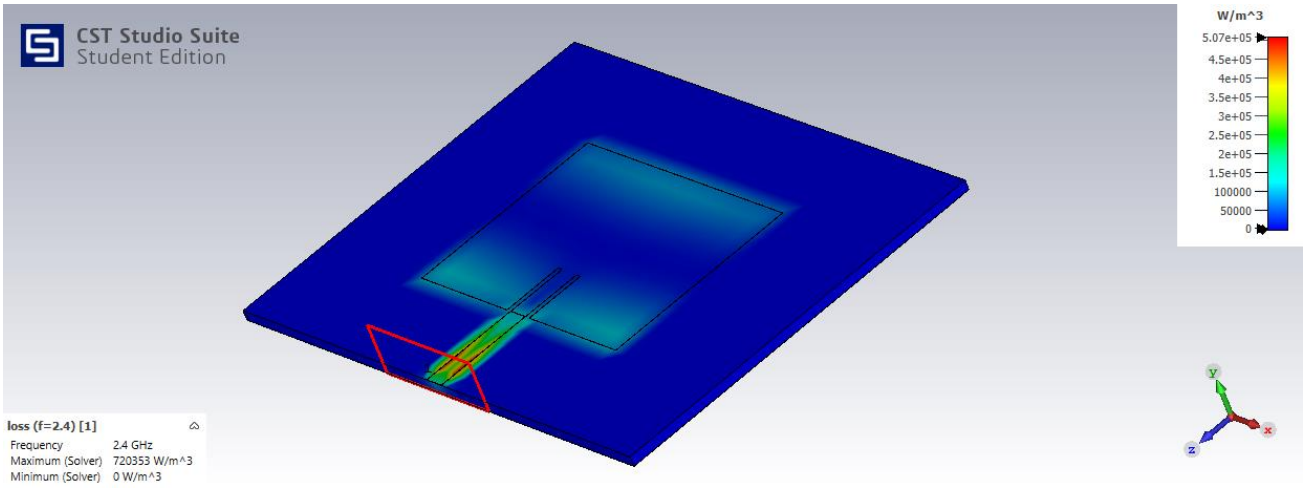

Fig: Power loss density(f=2.4)

The above figure shows Power Loss Density of microstrip patch antenna monitored at a resonant frequency of 2.4 GHz. It is observed that, near the feed line the power loss is not as much as it is on metallic patch. However, the power loss density is observed maximum at the surface of substrate or the dielectric material.

REFERENCES:

- https://easyengineering.net/
- https://www.worldscientific.com/doi/pdf/10.1142/9789813208605_0001
- https://www.technia.com/blog/what-is-cst-studio-suite/
- https://www.3ds.com/products-services/simulia/products/cst-studio-suite/latest-release/
- Google